Possibilities and limitations of exhaust gas analysis for expanded use in control of an AOD-converter

By

Jonas Laxén

Master of Science Thesis

Department of Materials Science & Engineering

Royal Institute of Technology

Stockholm 2012

KTH Industrial Engineering and Management

Examensarbete MSE 2012: MH200X 2012

Possibilities and limitations of exhaust gas analysis for expanded use in control of an AOD-converter

Jonas Laxén

Approved	Examiner	Supervisor
2012-month-day	Pär Jönsson	Patrik Ternstedt
	Commissioner	Contact person
	Outokumpu Stainless	Jyrki Pitkälä

Sammanfattning

Huvudsyftet med AOD-konvertern är att sänka kolhalten i produktionen av rostfritt stål. Kolhalten kan uppskattas av statiska teoretiska modeller. Den kan också uppskattas av dynamiska modeller baserade på analys av avgaserna från konvertern. Det här examensarbetet handlar om utvidgning av användandet av avgasanalysdata på AOD-konvertern på Outokumpus stålverk i Avesta, Sverige. Det finns i huvudsak två metoder för att bestämma kolhalten med hjälp av avgasanalys, massbalans och en linjär regression mellan kolfärskningshastigheten och kolhalten. Det här examensarbetet fokuserar i huvudsak på utvecklingen av den linjära modellen för stålsorterna ASTM 304L, 316L, S32101 och S32205 för sista steget i kolfärskningen. Samt stålsorterna ASTM S32205 och S30815 för näst sista steget i kolfärskningen. Resultaten visade att den linjära modellen kunde uppskatta kolhalten i sista steget av kolfärskningen med en standardavvikelse mellan 0,00626 %C och 0,0109 %C för de fyra olika stålsorterna. En ekvation som anger sambandet mellan sammansättningen på stålet under kolfärskningen och ekvationen för den linjära regressionen togs också fram i examensarbetet. Teoretiskt kan ekvationen användas för alla stålsorter men den har inte än blivit testad på andra stålsorter. CRE uppmätt med hjälp av avgasanalys undersöktes också för att ta reda på om CRE kan användas för att bestämma när stegbytena ska ske, det gick dock inte att utgöra från resultaten.

Nyckelord: Avgasanalys, rökgasanalys, dynamisk modell, kolhaltsmodell, AOD konverter, kolhalt.

KTH Industrial Engineering and Management

Master of Science Thesis MSE 2012: MH200X 2012

Possibilities and limitations of exhaust gas analysis for expanded use in control of an AOD-converter

Jonas Laxén

Approved	Examiner	Supervisor
2012-month-day	Pär Jönsson	Patrik Ternstedt
	Commissioner	Contact person
	Outokumpu Stainless	Jyrki Pitkälä

Abstract

The main purpose of the AOD-converter is to lower the carbon content in stainless steel production. The carbon content can be estimated by static theoretical models. It can also be estimated through dynamic models based on analysis of the exhaust gases from the converter. This master thesis is a study on an extended use of exhaust gas analysis data on the AOD-converter at Outokumpu's stainless steel plant in Avesta, Sweden. There are two main methods of predicting the carbon content based on exhaust gas analysis, mass balance and a linear regression between decarburization rate and carbon content. This master thesis mainly focuses on the development of the linear regression model for steel grades ASTM 304L, 316L, S32101 and S32205 for the last step of the decarburization, as well as ASTM S32205 and S30815 for the second last step of the decarburization. The results showed that the linear regression model can predict the carbon content at the last step of decarburization with a standard deviation between 0,00626 %C and 0,0109 %C for the different steel grades. An equation for carbon prediction dependent on the steel composition was also developed in the master thesis, making it theoretically possible to use for all steel grades, it has however not yet been tested on other steel grades. The CRE measured from the exhaust gases was also studied to find out if it is possible to use as basis for step changes during the decarburization, but the results were inconclusive.

Keywords: Exhaust gas analysis, off-gas analysis, dynamic model, carbon prediction model, AOD converter, carbon content.

Table of contents

1. Introduction

1.1 Background

The main purpose of the AOD-converter is to lower the carbon content in the steel. The process is monitored and controlled by a static theoretical mathematical model. The momentary carbon content in the steel as well as other alloying elements and the temperature are calculated by the static model. It uses input values such as starting composition, weight and temperature and how much gas that is blown in during the process. It then calculates the composition and temperature based on mass and heat balances and thermodynamics. There are, however, other factors which affect the process that the static model does not consider. For example, the age of the converter lining, dissolution of the refractory, etc. A dynamic model which predicts the carbon content based on analysis of the exhaust gases can to a greater extent consider the momentary conditions in the converter and work more reliably than a static model. Such a model has already been developed previously at Outokumpu's steel plant Avesta Works but for this master thesis a new sample point for analysis of the exhaust gases was installed. The new sample point is situated further away on the exhaust gas channel. It is believed to give more stable measurements and less fluctuations and the new carbon prediction model could therefore be more accurate.

1.2 Company description

Outokumpu is a major international stainless steel company. The group's head office is located in Espoo in Finland. Outokumpu's stock is registered on the NASDAQ OMX Helsinki in Finland. The company gets its name from the town of Outokumpu in Finland. In 1910 copper ore was found in Outokumpu and in 1932 the company Outokumpu was established to mine and process the copper ore in Outokumpu. During the 1950:s and 60:s Outokumpu opened nickel, copper and zinc mines in Finland. In the 1960:s the company opened a nickel plant in Harjavalta. In 1960 Outokumpu started exploitation of a large chromium ore deposit in Kemi in the north of Finland and constructed a ferrochrome smelter in Tornio near Kemi. Outokumpu then had both chrome and nickel production which are the main alloying elements for stainless steel and therefore started production of stainless steel. In 2000 Outokumpu adopted a new strategy which was to grow in stainless steel and sell off other businesses. In 2001 it merged with stainless steel producer Avesta Sheffield with production plants in Avesta, Sweden and Sheffield, England, forming a new company AvestaPolarit. Outokumpu bought AvestaPolarit in 2004 making it a fully owned subsidiary of Outokumpu. Today Outokumpu's main business is almost exclusively stainless steel. In the end of 2011 it had over 8200 employees in over 30 countries. The production was 1,391 million tons of stainless steel and sales were 5 billion euro.

The company made a net loss of 186 million euro. The company's biggest market was Europe which accounted for 75% of sales during 2011 [1][2].

On the 31:st of January Outokumpu and Thyssen Krupp announced a merger between Outokumpu and Thyssen Krupp's stainless steel unit Inoxum. Under the agreement Inoxum will be part of Outokumpu and Thyssen Krupp will acquire 29.9% of Outokumpu in a direct share issue [1].

1.3 The process route at Avesta Works

Outokumpu's stainless steel plant in Avesta is a scrap based integrated steel plant. An integrated steel plant is a steel plant where steel is produced from raw material, in this case scrap to finished, hot or cold rolled steel products. The different processes of the production at Avesta Works are shown in figure 1.3.1. The steel is then further processed in the rolling mill. Outokumpu buys scrap which is transported buy trucks or train to the scrapyard at the plant. In the scrapyard the scrap is analyzed and sorted according to composition in order to know the composition of the charged materials later on in the process [3]. The scrap is charged into buckets in the scrapyard from where they are transported to the electric arc furnace (EAF) [3].

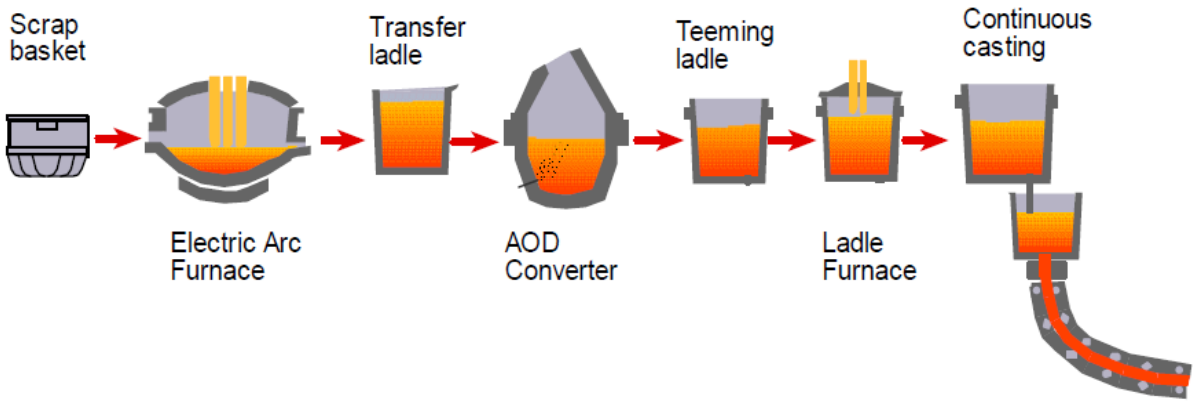

Figure 1.3.1: Illustration of the process route of stainless steelmaking at Avesta Works. The steel is afterwards further on processed in the rolling mill [4].

The scrap is melted in the EAF. It is charged with two or three buckets of scrap in order to fill it sufficiently. The charging weight is usually around 100 ton. The first bucket consists of scrap which may contain oil. It goes straight into the EAF because oil might ignite and form hazardous gases. The other bucket is preheated using the exhaust gases from the EAF [5]. Preheating removes moisture (either water or ice during the winter) from the bucket which otherwise could cause explosions in the EAF. The buckets also contain alloying elements. High carbon ferro chromium is usually loaded in the second bucket to achieve a high enough chromium content. High carbon ferro chromium is used due to its low price. Other alloying elements may

also be added to the bucket if the scrap's composition is far from the desired final composition. Ferro silicon is usually added through lances straight into the EAF to be used as a reduction agent [5].

The scrap is melted by three graphite electrodes. A current is applied in the electrodes which will cause an electric arc to form between the tip of the electrodes and the scrap. The temperature in the electric arcs can reach 10 000-30 000 °C and they have a maximum power of 90 MW [5]. The scrap is melted by heat radiation from the electric arcs. The heating, however is uneven and furthest away from the electrodes three cold spots are formed as can be seen in figure 1.3.2. These cold spots are heated by oxy-fuel burners to even out the temperature differences. Lances are used to inject elements into the EAF. Carbon powder, ferro silicon, oxygen and nitrogen are injected through lances to help create a foaming slag. Foaming slag helps to protect the refractory in the EAF from the intense heat. Water cooling is also used to cool the upper walls and the lid of the EAF. The temperature is estimated throughout the EAF process by a model and at the end it is usually measured by a robot. When the right temperature has been reached the melt is tapped from the EAF into a ladle. In the ladle the slag will be removed and a sample of the steel and slag will be taken. The result of the sample will be used as basis for process optimization in the next step which is the converter [3][5].

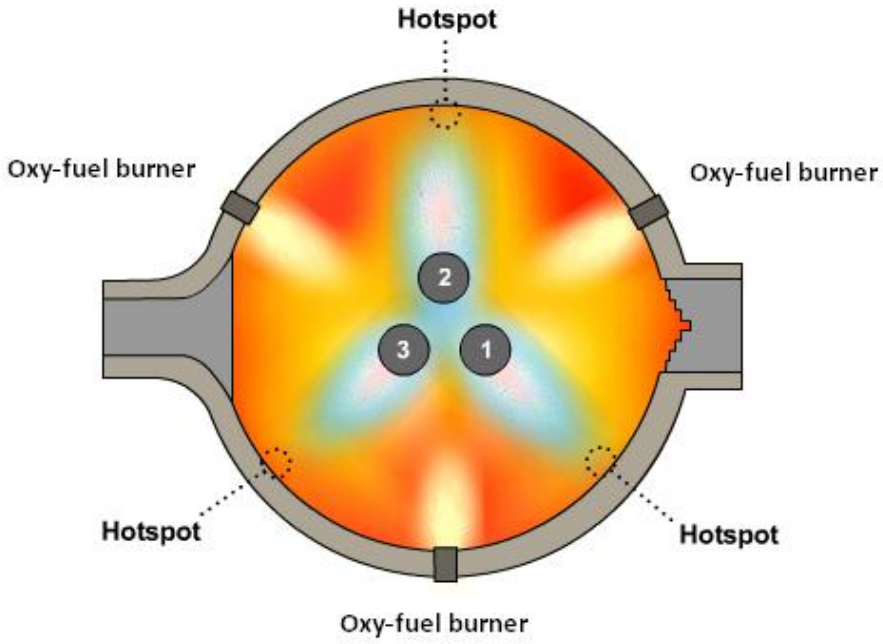

Figure 1.3.2: Illustration of the temperature differences in the EAF. Point 1, 2 and 3 represents the electrodes [5].

The converter used at Avesta Works is an argon oxygen decarburization converter, commonly known as an AOD-converter. It is a converter which is used for refining of stainless steel. The process in the AOD-converter is divided into three steps with the following purposes:

- Decarburization: Lower the carbon content in the melt.
- Reduction: Reduce oxides in the slag to regain valuable alloying elements.
- Sulfur refining: Remove sulfur.

The charge weight into the converter at Avesta usually varies in the interval 70-90 tons. Decarburization is achieved by blowing in oxygen and inert gas through 6 tuyeres placed on the sides. AOD-converters may also use a top lance for gas blowing, but it is not used at Avesta Works.

The converter does not have any external heating, it is only heated through exothermic reactions like the oxidation of silicon, carbon, chromium and other metals. In fact it requires cooling to avoid too high temperatures. Cooling scrap is added to cool the melt and to dilute it with respect to certain alloying elements if needed. The cooling scrap consists of reused internal scrap from the steel plant. Alternatively, if cooling scrap is not available synthetic material is added.

Throughout the AOD process there are many additions. Apart from additions to steer the process, some alloying additions are made in the converter in order to achieve the right composition.

Samples are taken during different steps of the AOD process. Sometimes a carbon sample is taken at the end of the decarburization period. A sample for all major alloying elements is always taken after the reduction and sulfur refining steps respectively.

At Avesta a software called UTCAS (Uddeholm Technology Converter Automation System) is used to optimize the process in the AOD-converter. It is a static model and uses the steel analysis from the sample before the converter as basis for the process. By heat and mass balances and thermodynamics it calculates how much gas should be injected and what material additions are needed. It gives the operators a schedule of how to run the process, when to make additions and change blowing steps and so forth.

During the decarburization oxygen reacts with dissolved carbon forming carbon monoxide which exits the converter as gas. The gas is sucked into the exhaust gas channel through the hood which is mounted over the converter. Inert gas, either argon or nitrogen is also blown in combination with oxygen during the decarburization. It is done in order to promote the decarburization by diluting the formed CO gas.

During the reduction and sulfur removal only inert gas is injected, mainly for stirring. The aim of the reduction step is to reduce oxides containing alloying elements, such as chromium, manganese and iron. It is achieved by adding a reduction agent, usually silicon because it is the cheapest alternative. After the reduction it is possible to start the sulfur refining step immediately with the same slag. However, it can also be removed and replaced with another type of slag which is more useful in the desulfurization. Depending whether or not the slag is replaced it is called one or two slag practice. In a two slag practice the slag from the reduction step is removed and burnt lime (CaO) is added to promote sulfur removal. At Avesta Works, a two slag practice is used. After the desulfurization excess slag is removed and the melt is tapped into a ladle. Some slag, is however kept because it works as insulation for the melt in the ladle furnace. The melt is then tapped into a ladle for further processing in the ladle furnace [3][5][6].

In the ladle furnace the melt is processed to achieve the right composition and temperature before casting and also to remove inclusions. Correct composition is achieved by adding alloying elements through either feeding bins or by wire feeding where the alloying element is in powder form inside a steel wire. The steel wire protects the powder and ensures that it goes through the slag and is then dissolved in the melt.

When the melt arrive from the converter to the ladle furnace the temperature steadily drops. To adjust the temperature the ladle furnace is equipped with three graphite electrodes to heat the melt.

To even out the temperature differences and remove inclusions the melt needs to be stirred. The ladle furnace is equipped with two kinds of stirring, inductive and inert gas stirring. Inductive stirring uses an electromagnet which is placed against the ladle. The electromagnetic field of the electromagnet causes the melt stir. It is also possible to change the power and direction of the field. Inert gas stirring uses a porous plug in the bottom through which argon gas is injected. The stirring homogenizes the melt and thereby evens out temperature differences and also helps to remove inclusions to the slag.

When the right composition and temperature has been reached and the inclusion content is low enough the steel melt is ready for casting and is placed on the ladle turret [5].

The steel is finally casted into slabs using continuous casting. The steel melt is first tapped from the ladle into a tundish. The tundish works as a buffer providing melt to the mold even when changing ladles. It also evens out the temperature and removes inclusions. From the tundish the steel melt is transported to the mold situated below through a casting pipe. The dimensions

of the slabs are finally decided by the mold. The mold cools the melt and the steel solidifies. A continuous feeding of melt allows long slabs to be casted. The slabs are then cut and sent to the rolling mill and for final treatment [5].

1.4 The AOD process

The AOD process is the dominating process for stainless steel refining, accounting for 72% of the stainless steel production worldwide [4]. With the introduction of the AOD-converter it was possible to use raw materials such as ferro chrome with a high carbon content because the AOD-converter effectively removes carbon. Before the AOD-converter was invented, purer raw materials had to be used, which made stainless steel making very expensive.

The AOD-converter's purpose is to refine raw steel produced by the EAF. The process is divided into three different steps, decarburization, reduction of top slag and sulfur refining all of which will be explained further below.

The main purpose of the AOD-converter is to lower the carbon content, it is done in the decarburization step. The carbon content in the melt from the EAF usually varies in the interval 1-3.5 %C [7]. The desired final concentration of carbon also varies from 0.2 %C to below 0.01 %C [4]. The high carbon content in the steel from the EAF is caused mostly by additions of high carbon ferrochromium. To remove carbon from the melt oxygen is blown in through tuyeres mounted at the sides in the bottom part of the converter and sometimes through a top lance. During the beginning of blowing mainly silicon, manganese and chromium are oxidized. The decarburization rate is then low but increases steadily as the silicon and manganese contents decrease and the slag gets chromium saturated [7]. Oxygen reacts with dissolved carbon according to equation (1):

$$\underline{C} + \tfrac{1}{2}O_2(g) = CO(g) \qquad (1)$$

The carbon monoxide exits the melt as gas and is sucked in to the exhaust gas channel through the hood which is situated over the converter. After exiting the melt the carbon monoxide will come in to contact with entrained air in the exhaust gas channel. The carbon monoxide will then react with oxygen in the entrained air and form carbon dioxide according to equation (2).

$$CO + 1/2O_2(g) = CO_2(g) \qquad (2)$$

Oxygen which is blown in will also react with dissolved chromium according to equation (3):

$$2\underline{Cr} + 3/2\ O_2(g) = Cr_2O_3(\text{in slag}) \qquad (3)$$

Both reactions are exothermic and increase the temperature in the converter.

The reactions (1) and (3) can be combined into one equation, equation (4).

Cr_2O_3(in slag) + 3C = 2Cr + 3CO(g) (4)

The equilibrium constant of (4) is expressed in equation (5) [7]:

$$\ln(K) = \ln(\frac{a_{Cr}^2 \cdot p_{CO}^3}{a_C^3 \cdot a_{Cr_2O_3}}) = -\frac{88704}{T} + 56.67 \quad (5)$$

Where a_{Cr} is the chromium activity, a_C the carbon activity, a_{Cr2O3} the chromium oxide activity and p_{CO} the partial pressure of CO.

To find the out how the equilibrium carbon content depends on other factors the equation can be rearranged as in equation (6).

$$\%C_{eq} = \frac{a_{Cr}^2 \cdot p_{CO}^3}{a_{Cr_2O_3} \cdot e^{\left(\frac{-88704}{T} + 56.67\right)} \cdot f_C} \quad (6)$$

Where f_C is the activity coefficient of carbon.

As can be seen from equation (6) a low equilibrium carbon content is promoted by a:

- Low chromium activity
- Low partial pressure of CO
- High activity of chromium oxide
- High temperature
- High carbon activity coefficient

It is not possible to do anything about the chromium activity and the carbon activity coefficient since the final composition demands high amounts of chromium and other elements. The chromium oxide activity in the slag will stay close to unity due to low solubility in typical AOD slags. The temperature cannot be increased too much because it would increase the wear of the converter. The partial pressure of CO however can be lowered through dilution with inert gases. This is a technique which is used in the AOD process. Oxygen is blown in combination with inert gas, either nitrogen or argon. At the beginning when the carbon content is still high, only little dilution is needed. As the carbon content decreases a lower partial pressure of CO is needed and therefore greater dilution with inert gases. Dilution will result in a higher carbon removal efficiency (CRE) which is defined according to equation (7):

$$\mathrm{CRE}(\%) = \frac{\text{Amount of oxygen reacting with carbon}}{\text{Total added oxygen}} \cdot 100 \quad (7)$$

A high CRE number is desirable. A CRE of 100 would theoretically mean perfect efficiency but it may reach values of more than 100 sometimes when changing steps. This may be due to dissolved oxygen which contributes to the decarburization. Moreover, when only inert gas is blown dissolved oxygen will react with carbon. Since there is no blowing of oxygen the CRE would be infinite. The technique of blowing in steps with different ratios between oxygen and inert gas helps to increase the CRE. An increase in CRE does, however, not mean an increase in decarburization rate. The efficiency of used oxygen will increase but the decarburization rate might decrease due to a lower amount of oxygen. It does however mean that less alloying elements will be oxidized which is highly beneficial. The CRE is high at the beginning of each step, and then decreases until the next step change. Figure 1.4.1 shows how the CRE varies during the process, with the sudden rises indicating a step change [4]. In the beginning of the process mainly silicon, manganese and chromium is oxidized and the CRE is therefore low. But as the silicon and manganese contents decrease and the slag is saturated on chromium, the carbon starts to oxidize and the carbon removal efficiency increases. During the decarburization chromium and manganese slows down the decarburization rate while the more noble alloying elements nickel and molybdenum increases it. The decarburization rate therefore partly depends on the steel composition.

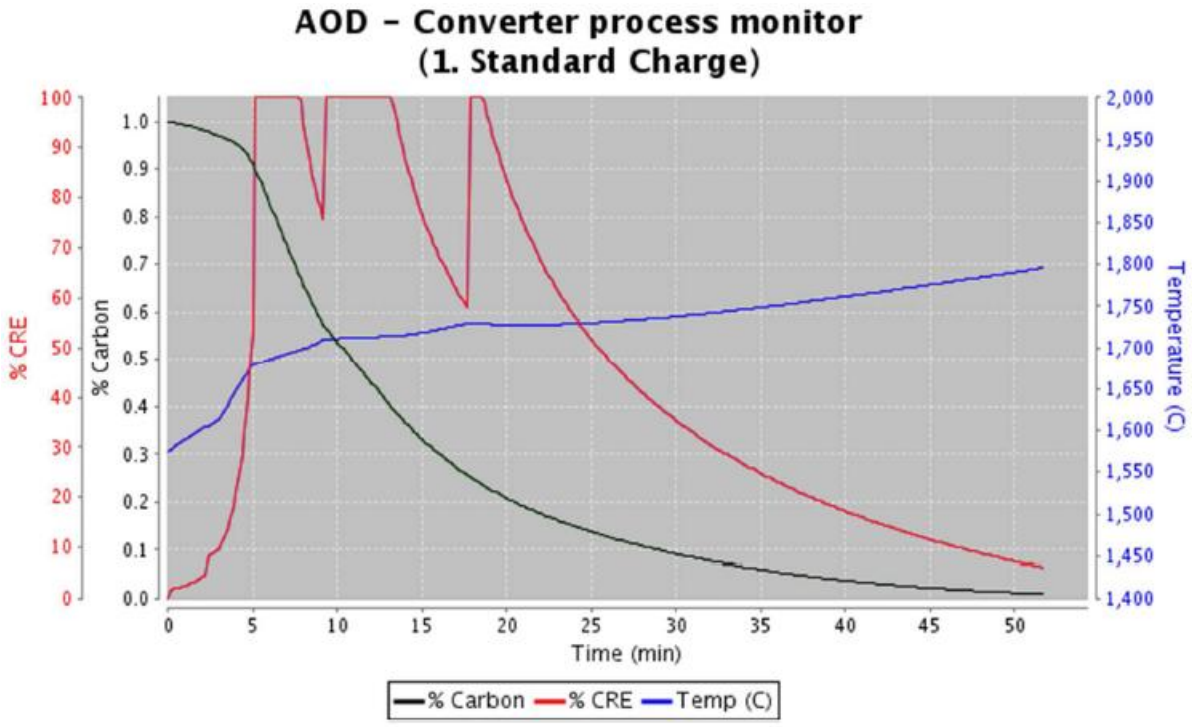

Figure 1.4.1: A plot of the carbon content, temperature and CRE during the decarburization. It is based on theoretical calculations and not actual measurements. The plot indicates that there are three blowing steps, in Avesta Works however four different steps is the most common [4].

The gas blowing is done in steps. In the first step the ratio between injected oxygen and inert gas is high. But as the carbon content decreases each following step has a lower ratio, meaning less oxygen and more inert gas, in order to lower the partial pressure of CO. When to change steps is decided by two conditions. It is changed either at a specific carbon content or temperature calculated by UTCAS. When the carbon content is sufficiently low the decarburization is ended. In order to find out if it is low enough a carbon sample is sometimes taken at the end of the last step at Avesta Works. Other times the operators at the converter rely on the carbon prediction model developed prior to this master thesis. However, the model is not accurate enough and the operators therefore often end the step when the model indicates a lower carbon content than the desired final content to be on the safe side. Carbon can rather easily be added later while if it is too high redecarburization would be needed. Charges with carbon contents higher than expected are referred to as having a slow decarburization at Avesta Works. Charges with lower carbon content are on the other hand referred to as having a fast decarburization. Today there is no way of predicting a slow or fast decarburization. The static model also predicts the carbon content and decides when to change steps. However, it is too inaccurate to determine when to end the decarburization.

The rate limiting mechanisms of the decarburization are one of the following:

- Supply of oxygen to the melt
- Carbon activity and CO partial pressure in the melt
- Diffusion of carbon at the boundary layer of the gas bubbles

In the beginning when the carbon content is high the supply of oxygen is rate limiting. At lower carbon contents one of the two last mechanisms is rate limiting [7].

The reduction step follows the decarburization. The purpose of the reduction is to reduce oxides in the slag to obtain a higher yield of alloying elements, especially chromium oxide reduction is important. A reduction agent, either silicon or aluminum is added. Silicon and aluminum have higher oxygen affinity than chromium and it is therefore possible to reduce the chromium oxide. Silicon is cheaper than aluminum and is therefore often preferred. Furthermore, aluminum forms a type of hard inclusions which may be harmful. However aluminum lowers the amount of oxygen in the melt more than silicon and is therefore sometimes used when low sulfur contents are required. Silicon is added in the form of ferrosilicon [7]. The reduction reaction by silicon is expressed in equation (8).

$$Cr_2O_3(\text{in slag}) + 3/2\ \underline{Si} = 2\underline{Cr} + 3/2SiO_2(\text{in slag}) \qquad (8)$$

The kinetics is favored by stirring. The converter is therefore stirred by injection of inert gas during the reduction. After the reduction, sulfur refining is carried out.

The purpose of the sulfur refining is to decrease the sulfur content in the steel. At Avesta Works two slag practice is used. A slag-off is first performed to remove the slag from the reduction. Burnt lime (CaO) and fluorspar (CaF_2) are added to provide a favorable slag for sulfur removal [4][7]. Sulfur is removed according to equation (9).

$$CaO + S = CaS + O \quad (9)$$

1.5 Objective

The aim of the master thesis is to develop one or several models based on exhaust gas analysis for the AOD-converter. The model/models should provide information to help decision making on when to change steps or finish the decarburization. A new sampling point has been installed before the master thesis and the model should use measurements from it instead of the old position. The new model should be valid for more steel grades than the existing one and should if possible work reliably in additional steps of the decarburization. The tasks in the master thesis are to:

- Find out what models exist through a literature study
- Develop a model
- Evaluate which sample point gives the most reliable measurements
- Evaluate the accuracy of the model
- Calibrate the parameters in the model through experimental data
- Evaluate which new parameters possibly would be needed to improve the model
- Develop guidelines for when the model can be used reliably

1.6 Benefits of exhaust gas analysis

With a successful exhaust gas analysis the operation time in the AOD-converter could be shortened. A greater efficiency regarding injected gas and material additions could also be achieved. With a successful model, the need for the carbon sample during the decarburization could be eliminated or at least reduced. Thus saving a few minutes per charge compared to if the carbon sample was taken. It could also help the operators to determine when to change steps. It could then be avoided to change steps too late or too early. This would ultimately result in a more efficient decarburization. An efficient decarburization would mean less use of injected gas, less oxidation of alloying elements and a faster decarburization. The reduced use of gas and saving of alloying elements would reduce costs and a faster decarburization would increase production and thereby earnings. Today, the converter is the bottleneck in the production at Avesta works [4]. Therefore a shortened process time could increase the plants total output of steel.

2. Literature study

A literature study was conducted in order to find out what models for exhaust gas analysis exist and to learn more about the process and measuring equipment. The literature which was studied in this master thesis consisted of the old master thesis report, the reports referenced in it and internal documentation on the development of the exhaust gas analysis at Avesta Works. It also included reports on the implementation of an exhaust gas analysis at Outokumpu's plant at Tornio in Finland. The literature study also included a search for scientific reports on the internet. Several reports were found through the reference database Metadex, which is specialized on material science. Other reports were ordered from Jernkontoret, the Swedish trade organization for steel.

The literature study indicated that there are two techniques for carbon prediction in the AOD-converter by exhaust gas analysis. One is the method of finding a linear correlation between the decarburization rate and the carbon content, which from here on will be referred to as the linear regression model. Thereby, predicting the carbon content based on the decarburization rate which is measured from the exhaust gas analysis. The other method is to calculate the carbon content through a mass balance for carbon.

The linear regression model is today in use at Outokumpu's plants in Avesta and Tornio. In the next section "Earlier work" 2.1 the model used in Avesta Works is described in detail. Tornio's carbon prediction model was developed in 1992, before the one in Avesta. It was developed in a similar fashion to the one in Avesta focusing only on the last step of the decarburization. The exception is that it does not use a V-cone for gas flow measurements. It instead relies on gas balance calculations for the flow rate.

The other method is to use a mass balance for carbon. In the mass balance it is calculated how much carbon goes into the converter and how much exits it. The amount of carbon in to the converter is calculated on basis of the steel sample after the EAF and weighing of the steel melt. The steel sample gives the carbon content in the steel melt and when it is multiplied with the weight of the steel melt the mass of carbon in the steel melt into the converter is acquired. Carbon is also added during the process which needs to be considered in the calculations. The amount of carbon in can be expressed according to equation (10).

$$m_{C_{in}} = \frac{\%C_{Fe} \cdot m_{steel}}{100} + m_{Cadditions} \qquad (10)$$

Where m_{Cin} stands for the carbon mass in the steel melt into the converter, $\%C_{Fe}$ the initial carbon content in the steel, m_{steel} the initial steel weight and $m_{Cadditions}$ the carbon mass from additions to the converter during the process.

Carbon exits the melt in form of either CO or CO_2. By measuring the gas flow and composition of the gas, it is possible to calculate how much carbon is removed per time unit. By integrating it the amount of carbon removed during the time period is achieved as can be seen in equation (11).

$$m_{C_{out}} = \int_0^t \left(\frac{dC}{dt} \cdot dt \right) \tag{11}$$

Where m_{Cout} stands for the mass of carbon which exits the converter in gas form and dC/dt stands for the decarburization rate.

By subtracting the weight of carbon in with the weight of carbon out you get the amount of carbon in the melt and when divided with the steel weight the carbon content is acquired according to equation (12).

$$\%C_{Fe} = \frac{m_{C_{in}} - m_{C_{out}}}{m_{steel}} \cdot 100 = \frac{\frac{\%C_{Fe} \cdot m_{steel}}{100} + m_{C\,additions} - \int_0^t \left(\frac{dC}{dt} \cdot dt \right)}{m_{steel}} \cdot 100 \tag{12}$$

Several studies have been conducted with the aim of developing a reliable model based on mass balance for carbon in order to predict the end carbon content. However, from the literature study it seemed none of the attempts were successful. An attempt by Mikael Lindvall et al. at Avesta Works yielded an error mean value of -0.003 %C and a standard deviation of 0.097 %C [8]. Another attempt by C. Burkat et al. at Krupp Thyssen Nirosta's plant in Bochum yielded a mean value ratio between calculated and actual carbon content of 1.001 and a standard deviation of 5.7 % of the start weight of carbon [9]. For a standard charge it resulted in a standard deviation of 0.091 %C. Both used adjusting parameters in the calculations of dC/dt using information from previous charges to smooth out errors. Mikael Lindvall et al. used equation (13) for calculating dC/dt:

$$\frac{dC}{dt} = \frac{v_{tot} \cdot \left(\%CO + \%CO_2 \right) \cdot M_C \cdot 1000 \cdot CF}{100 \cdot 60 \cdot V_{STP}} \tag{13}$$

Where %CO and $\%CO_2$ stands for the percentage of CO and CO_2 gas in the exhaust gases, v_{tot} the flow rate of the exhaust gases, M_C the molar mass of carbon, V_{STP} the volume of 1 mole gas at standard conditions and CF stands for correction factor. It was calculated as the average value of all charges in the study.

This could practically eliminate the mean error value and slightly reduce the standard deviation but it still remains high. From this it is evident that the reliability of the mass balance model is too low to determine the end carbon content. Since the standard deviation is even several

times higher than the final carbon content itself in most steel grades. The reason for the large standard deviation is that each new iterative calculation in the model is based on a previous value, meaning that errors propagate through the model. An error of a few percent in the beginning when the carbon content is 1-2.5 %C will cause a too big error in the end. For a charge of start weight 85 ton and a carbon content of 2 %C an error of just 1% would result in a deviation of 0.02 %C. This makes the mass balance model too sensitive to measurement errors since it relies heavily on precise measurements but many of the measurements in the AOD-converter are far from precise. Many of the measurement equipments have a precision interval of 1%. Many simplifying assumptions are also needed in the calculations which probably result in some error.

A report by Pentti Kupari states that the linear regression model used in Tornio and Avesta based on the decarburization rate only has potential to work sufficiently well for the last two steps. When the carbon content is high it is too unreliable. According to him, another type of model is needed for the first two steps [10].

2.1 Previous work

Three previous projects on exhaust gas analysis have been carried out at Avesta Works. The first was conducted in the mid 1990:s using a system called Mefcon developed by Mefos. Mefcon is an advanced program which calculates mass and heat balances using some online measurements. It calculates the carbon content by mass balance using exhaust gas analysis. The trials with Mefcon at Avesta Works however showed that it could not predict the carbon content with high enough precision during a study in 2002. The carbon content could be predicted with an accuracy of ±0.025 %C in 50% of the cases and with ±0.05 %C in 85% of the cases [11]. The precision when considering all of the cases have not been documented. According to the master thesis project from 2003 however, the Mefcon system worked satisfactorily as long as it had fast enough computers to support it. Mefcon did not have its own CPU, but had to share it with other systems. When the other systems used too much of the CPU's capacity it either disturbed the Mefcon calculations or caused it to crash. However, no information on the accuracy or references was provided [12].

In 2003 a master thesis on exhaust gas analysis was conducted. The purpose of the project was to develop a model which predicts the carbon content in the AOD-converter during the last decarburization step for certain steel grades based on exhaust gas measurements. The steel grades included in the study were ASTM 304L, 321 and 316 Ti. Carbon samples were taken from the converter during the last steps of the decarburization. For 304L samples were taken during step 3 and 4 and for 321 and 316 Ti samples were taken during step 2,3 and 4. The carbon content was then compared to the decarburization rate dC/dt at that time. It was assumed that there is a linear relation between the carbon content and dC/dt. An equation of how the carbon

content depends on the decarburization rate was estimated from the data acquired from the samples, one equation for steel grade 304L and one common equation for 321 and 316 Ti. It was found that the model was too inaccurate when including step 3 and 2. The model was therefore only developed for the last step, step 4 but the author concludes that one separate model for each step could be more successful. The accuracy in the model used for 304L was 0.01 %C. Steel grades 321 and 316 Ti share the same equation and the accuracy of it was found to 0.018 %C. The author does not mention in the report how the accuracy was calculated but it is likely the standard deviation. The method of measuring the gas flow was also investigated. The precision of the V-cone was compared to the method of calculating the gas flow through gas balance calculations. The V-cone was found to be the most accurate [12].

In 2006 an attempt by Lindvall et al. on developing a mass balance model for carbon prediction was done at Avesta as mentioned previously in the literature study section. One purpose of the project was to be able to use the carbon prediction model as basis for step changes. However, the project was unsuccessful. The model was not enough accurate to use as a basis of when to change steps, probably due to the fact that the measurements were not accurate enough [8][11].

3. Experimental

In order to develop the carbon prediction model for the new sample point carbon samples needed to be taken for the selected steel grades.

3.1 Steel grades

The steel grades included in the study were the following: Standard stainless austenitic steels ASTM 304L and ASTM 316L, duplex stainless steels ASTM S32101 and ASTM S32205 and the high carbon stainless austenitic steel ASTM S30815. The composition of the steel grades can be seen in table (3.1.1)

Table 3.1.1: The table displays the compositions of the steel grades in the study. The contents given in the table are the aimed contents. In the production there is also an interval of acceptable alloying element contents [13].

Steel grade	Cr (wt.%)	Ni (wt.%)	Mn (wt.%)	Mo (wt.%)	C (wt.%)	Si (wt.%)	N (wt.%)
304L	18,2	8,1	1,7	0	0,021	0,35	0,065
316L	17,1	10,1	1,6	2,07	0,023	0,55	0,045
S32101	21,5	1,55	5	0,3	0,025	0,7	0,22
S32205	22,4	5,7	1,5	3,2	0,018	0,4	0,17
S30815	20,95	10,95	0,55	0	0,09	1,7	0,165

3.2 Sampling criteria

The carbon samples were taken during the end of step 4 for steel grades 304L, 316L, S32101 and S32205 and at the end of step 3 for steel grades S32205 and S30815. The aim was to get a spread of carbon samples during the end of step 3 and 4. The samples were taken at the end of each step because the model needs to precise in the end of the step in order to know when the step should be finished. It is not as important for it be accurate in the beginning of the step since no decisions will be made based on the model at that time.

3.3 Preparations

During the start of the master thesis all the necessary equipment for the new sample point was installed but it had not been used or tested. For the gas composition measurements the old mass spectrometer and a new IR-spectrometer would be used. The hose from the old sample point was removed from the mass spectrometer and simply replaced with the hose from the new sample point. This enabled the mass spectrometer measurements from the new sample point to be stored without any changes in settings. However, the new IR-spectrometer required some configuration before the measured values could be stored. When the measurements from the new sample point, both from the mass spectrometer and the IR-spectrometer were stored automatically the sampling in the AOD-converter began.

4. Measuring equipment

4.1 Gas extraction

To analyze the composition of the gas in the exhaust gas channel, continuous gas samples are needed during the decarburization. At Avesta works an extractive technique for gas sampling is used. Sampling gas is extracted from the exhaust gas channel through a probe and the gas is lead through a hose to the analysis room.

The old sample point at Avesta was located approximately 25 m away from the converter and its position can be seen on figure 4.1.1. For this project a new sample point was installed. The new sample point is located on the roof of the converter building, 65 m away from the converter as can be seen in figure 4.1.1. It is situated a few meters before the V-cone. It is believed that the new sample point will yield a more stable analysis of the gases [3][14]. CO gas which exits the converter will react with oxygen from entrained air and form CO_2 which will generate heat. It is believed that this causes the measurements to fluctuate more. When analyzing the gas further away in the exhaust gas channel it is believed that less reactions take place. This should yield more stable measurements. However, by moving the sample point further away the response time for the measurements increase by approximately 20 seconds [3][14].

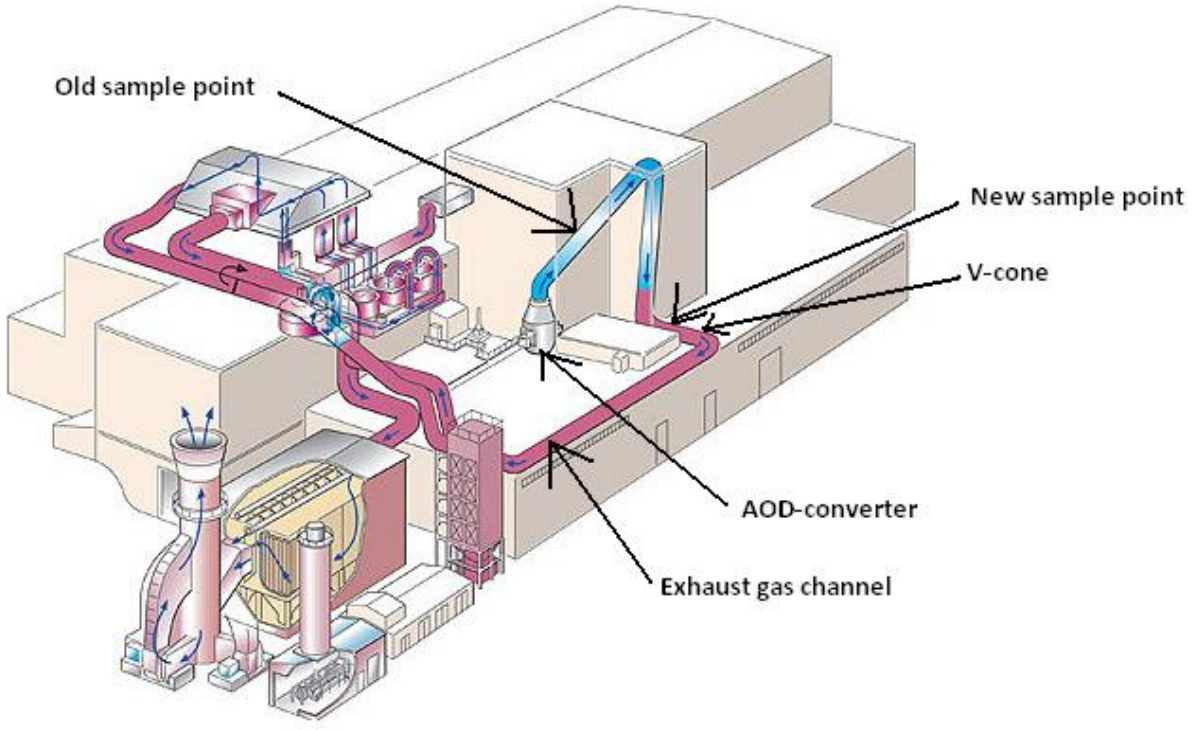

Figure 4.1.1: Illustration showing the AOD-converter, exhaust gas channel and sampling points. Note, the AOD-converter is not situated on the roof but below and the picture is not exactly according to scale [5].

In the new sample point gas is firstly extracted from the center of the exhaust gas channel by the probe. At the end of the probe there is a wider cylindrical space where the gas has to pass a filter before it is sucked out in a hose. There are two hoses leading in for clean blowing. One is situated in the same cylindrical space as the filter and is used to keep it and the outside of the filter clean of dust. The other one is situated on the other side of the filter and is meant to clean the filter from within. At the time of the master thesis the clean blowing was not automatic. It had to be done manually.

The gas is lead from the sample point to the gas analysis room through the hose which is heated to avoid condensation of water vapor in the gas. If the water vapor would condensate inside the hose it could cause the dust in the gas to clog the hose and thereby prevent gas from being analyzed. When the gas enters the gas analysis room it first goes into the water separator to dry the sample gas. The water separator cools the gas in two different heat exchangers which causes the water vapor in the gas to condensate. It is necessary to avoid moisture from entering the analysis equipment. It then passes through two filters to remove remaining dust. First one rough filter followed by a finer filter. The filters are white and turn yellow or brown when they have picked up dust, meaning it is possible to see on the outside if the filters need to be changed. After the filters the hose goes into the pump. It is this pump which is used to suck gas all the way from the probe. From the pump another hose goes out to the water separator again. The gas in the outgoing hose is pushed forward by the pump. After entering the water separator for a second and final time the hose goes to a moisture alarm, which stops the pump if any moisture is detected in order to protect the analysis equipment. After the moisture alarm, the hose goes through a flow indicator which indicates the gas flow rate in the sample hose. The hose then enters the IR-spectrometer and after the IR-spectrometer it finally enters the mass spectrometer.

During the trials after installing the new sample point dust entered the system and caused longer delays for the gas analysis. The first heat exchanger in the water separator became full of dust and dust was also visible in the hose. In the old sample point the gas first passed a filter in the analysis room before entering the water separator and then later passed another filter again. The configuration of the old sample point worked well and the heat exchangers were clean of dust.

4.2 Mass spectrometer

The mass spectrometer is used to measure the composition of the exhaust gas. At Avesta Works it is used to measure the concentration of argon, oxygen, nitrogen, carbon dioxide and carbon monoxide. However, in the carbon prediction model the measured value from the IR-spectrometer is used for carbon monoxide as it has proven more reliable. The reason for this is

that the CO and N_2 molecule has almost the same mass and the mass spectrometer has problems to distinguish them from each other. The advantages of mass spectrometers are the possibility to measure complex gases, the measurement sensitivity and a broad measurement interval. It is possible to measure concentrations from 0% to 100% [12]. The mass spectrometer has an estimated margin of error of 1% [8]. The measurement error is however proportional to the measuring range. To limit the measuring range to a minimum could therefore increase the accuracy [8].

Mass spectrometers work on the principle of separating ions according to their mass charge ratio m/z. In order to do this the gas has to be ionized first. It is done in an ionization chamber. The ionized gas then enters a chamber where it is accelerated through a magnetic field. The magnetic field will cause the ions to deflect at different curves depending on their mass charge ratio m/z. At the other end of the chamber a detector is located. Only ions of a certain m/z will reach the detector because the ions will deflect at different curves. The magnetic field can be varied and thereby it is possible to choose what molecules to analyze. When the ions hit the detector a small current will be created. This current is then amplified and the intensity of each component is registered. From the intensity the composition of the gas is then calculated by the mass spectrometer's software [12][8][15][10].

4.3 Infrared spectrometer

The IR-spectrometer is currently used at Avesta Works to measure the carbon dioxide and carbon monoxide concentrations in the exhaust gas. Only the IR-spectrometer's carbon monoxide measurements are however currently used in the carbon prediction model. It is suggested in the literature that measuring with the IR-spectrometer at low carbon dioxide levels would improve the accuracy of the measurements [8]. This is due to the fact that the precision of the measurement is dependent on the measuring interval and the mass spectrometer is used to measure in a much larger interval than the IR-spectrometer. The IR-spectrometer at Avesta Works' measuring range is 0-0,3% for CO and 0-0,1% for CO_2 [15][16].

Infrared spectrometers work based on the absorption of electromagnetic waves. Electromagnetic waves with an energy that corresponds to the energy quantum between different energy levels of rotation, vibration or electrons can be absorbed. These energy quantums are unique for each atom and molecule. It is possible to transmit light of such a certain wavelength through the gas and detect how much is absorbed. Then it is possible to calculate how much the specific atom or molecule absorbed by comparing the transmitted and detected intensity. From the measurement the IR-spectrometer's software calculates the concentration of the component. IR-spectrometers are divided into three categories based on the wavelength of the infrared light, near IR (NIR), middle Ir(MIR) and far IR(FIR). The IR spectrometer at Avesta Works uses MIR with wavelengths between 2.5-8 µm. The linearity

deviation for Avesta Works' Ir-spectrometer is less than 1% according to the manufacturer [16]. It calibrates itself once every other week [3][15].

4.4 V-cone

To measure the flow rate of the gases in the exhaust gas channel at Avesta Works a V-cone differential pressure meter is used. It is a flow meter device which can be used to measure a large variety of liquids and gases and is used in many completely different industries. The V-cone is shaped like a tube with a cone inside as can be seen in figure 4.4.1. The pressure is measured in the tube before the cone and at the cone. From that it is possible to calculate the flow rate by using Bernoulli's equation for conservation of energy in a closed pipe. The signals from the measurements are sent to the flow computer which calculates the flow rate. The flow rate at Avesta Works is given as kilo normal cubic meters per hour (kNm^3/h). The V-cone requires calibration for high precision measurements. The V-cone at Avesta Works has however not been calibrated. The flow computer can characterize a nonlinear calibration. Then the V-cone's measurements only need to be repeatable. The V-cone's repeatability is ±0.1% according to the manufacturer [17].

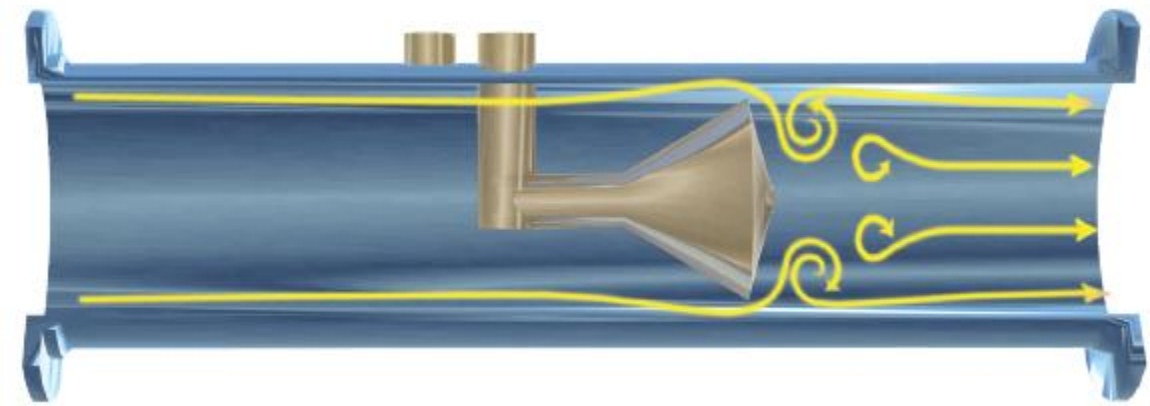

Figure 4.4.1: Illustration of a v-cone flow meter [18].

4.5 Alternative measuring techniques

There are currently techniques available and under development for measuring the exhaust gases' composition directly in the exhaust gas channel. One such existing technique is the tunable diode laser absorption spectroscopy (TDLAS). TDLAS works similar to IR-spectrometers, but instead of using large IR-spectrums it uses narrow absorption lines to identify each element. It has a fast response time and can withstand high temperatures, but it needs flushing of inert gas to keep the optical window clean from the exhaust gas, which makes it an expensive technique. Another promising method which is under development is microwave spectroscopy. It has fast response times and can operate in aggressive environments with high amounts of particles in the gas [15].

Measuring the gas composition directly in the exhaust gas channel would eliminate the need for gas extraction and thus greatly increase response time. The time of the gas extraction from the probe until when the IR-spectrometer gives a result has been measured to approximately 40 seconds. Therefore online measurements could save approximately 40 seconds in response time, meaning the delay would only be approximately 20 seconds.

4.6 Carbon samples

Carbon samples from the converter are taken as lollipop samples. Firstly the blowing has to be stopped and the converter tilted. The operators then manually stick in a pole with the sampler on the top through a hatch in the converter. The sampler is a cavity in the shape of a lollipop. The sample is then cooled and solidifies and is turned in for analysis at the laboratory. In normal production the temperature is also measured simultaneously with the sampling.

4.7 Sample analysis

The carbon samples are analyzed by a C/S-analyzer. It consists of one heating and one analysis unit. The samples are first incinerated in oxygen atmosphere inside the heating unit. Carbon is then oxidized to CO_2 which is measured by IR-detectors in the analysis unit. Based on the CO_2 measurements the carbon concentration in the sample is calculated. The accuracy of the carbon sample analysis has been statistically determined to be ±0,002 %C for carbon contents between 0,002 and 0,03 %C and can be expressed by equation (14) at higher carbon contents [19].

$$y = 0{,}0178 \cdot (\%C) - 0{,}0004 \qquad (14)$$

Where y is the accuracy.

5. Method and theory

In order to know which sample point gives the most accurate exhaust gas analysis both the new and old sample points were evaluated.

The samples were evaluated through charge data. Data consisting of the result of the carbon sample and the decarburization rate at the moment were compiled in Excel. From this information dC/dt could be plotted versus the carbon content and the correlation between dC/dt and the carbon content was calculated. The accuracy of the equation could then be estimated by calculating the standard deviation. dC/dt was also compared to the carbon activity in order to find out which method gives the most reliable predictions. To calculate the activity, the contents of the other alloying elements were needed. However, no samples of other elements than carbon were taken. UTCAS estimated contents were therefore used when calculating the activity.

The old sample point was evaluated through old charge data before the new sample point was installed. Charges that had a carbon sample were selected and analyzed. This was done for steel grades 316L, S32101, S32205 and 310S. No carbon samples were taken specifically for this. Only charges where carbon samples were taken as part of normal operation were analyzed. For steel grades 316L, S32101 and S32205 the carbon samples were taken during the last step while it was taken during step 3 for grade 310S. Only charges after the V-cone had been changed in the summer of 2011 were analyzed. For steel grade 304L there were not enough samples to evaluate it. High carbon steel grade 310S was evaluated instead of S30815 because at the time it had not yet been decided that S30815 would be included in study on the new sample point.

The measured CRE was also investigated. Charges which had a slow and fast decarburization were compared against each other. It was believed that if previous blowing steps were ineffective or terminated too early, it would result in a higher carbon content than expected i.e. slow decarburization in the last step. The efficiency of the first step is by far the most important step since it has the highest oxygen flow rate and the largest amount of carbon is oxidized in this step. The CRE of the first step was therefore investigated and compared for charges with slow and fast decarburization.

The mass balance model was also investigated. It has previously been proven to be not enough accurate for determining the final carbon content. However, it is unclear whether it can be used to determine the carbon content at the end of earlier steps when information from previous charges is known. In this maser thesis the mass balance model developed by Mikael Lindvall et al. was used. In Mikael Lindvall et al.'s study the correction factor was calculated as the average of all charges. In this master thesis it was investigated if using the correction factor from the previous charge on the next charge could increase the accuracy. The correction factor was

calculated using information from the charge data files for all steel grades and all charges. For charges of steel grade S32205 with carbon samples at step 3 the accuracy of the mass balance model was evaluated.

The measured contents of CO and CO_2 gas in the exhaust gas channel during the decarburization were plotted for both the new and old sample points. For the new sample point, the CO_2 content in the plot was measured by the mass spectrometer and the CO content by the new IR-spectrometer and both values were stored automatically. For the old sample point, the CO_2 content was measured by the mass spectrometer and the CO content by the old IR-spectrometer. For the old sample point the measurements by the mass spectrometer were stored automatically but the CO measurements by the IR-spectrometer were written down manually with 10 seconds interval to avoid needing to make electrical installations.

5.1 Calculations

The decarburization rate is calculated from the measured values of the exhaust gas flow rate, composition of exhaust gas regarding CO and CO_2 and a set of constants. The decarburization rate is expressed according to equation (15) [8].

$$\frac{dC}{dt} = \frac{v_{tot} \cdot (\%CO + \%CO_2) \cdot M_C \cdot 1000}{100 \cdot 60 \cdot V_{STP}} \qquad (15)$$

Where:
dC/dt = Decarburization rate (kg/min)
v_{tot} = Total flow rate of the exhaust gas measured by the V-cone (kNm^3/h)
%CO = Carbon monoxide content in the exhaust gas measured by the IR-spectrometer (%)
$\%CO_2$ = Carbon dioxide content in the exhaust gas measured by either mass spectrometer or IR-spectrometer (%)
M_c = Molar weight of carbon in CO and in CO_2 (g/mol)
V_{STP} = Gas volume of 1 mole of gas at standard pressure and 0 °C (dm^3/mol)

The expression is multiplied by 1000/60 in order to change the unit of v_{tot} to Nm^3/min. It is divided by 100 in order to change the percentage of CO and CO_2 into fractions.

5.2 Measurement delay

It takes time from the moment when the CO and CO_2 gas exits the converter until it is analyzed. After the gas exits the converter it has to travel 65 m to the sample point. From the sample point it then needs to travel to the gas analysis room and through many components before it finally reaches the analysis equipment. This will result in a delay of the measurements.

The best way to measure the delay was found in connection with the carbon sample when the converter is tilted and all blowing is stopped. Another way to measure the delay is to look at the start of blowing in the beginning of the process, but it was found to be unreliable.

The delay was measured by comparing the time between the start of inert gas blowing and when the CO_2 content measured by the IR-spectrometer began to rise. Inert gas blowing always starts before oxygen blowing, which means that the initial rise in CO_2 is due to the stirring effect of inert gas. If the delay was compared to when oxygen blowing was started instead, it would be difficult to see when oxygen starts to have an effect on the CO_2 content. Also, sometimes after the carbon sample oxygen blowing is stopped.

At the beginning of the trials with the new sample point the delay was found to be 1 minute and 10 seconds if the sample point had been blow cleaned. The measurements are stored with 10 second intervals so the delay could only be measured with 10 seconds accuracy. If the sample point had not been cleaned for a long time the delay would increase, usually after 8 hours of operation. After a few weeks however the delay started to increase even after blow cleaning. It was found that the first heat exchanger in the water separator was full of dust and there was also some dust in the hose leading to the heat exchanger. The problem was thought to be with the blow cleaning hoses and was corrected. The hoses to the heat exchangers in the water separator were redirected so that they entered the clean one first and later the dirty one. This resulted in the clean heat exchanger also becoming dirty from dust but it still performed well without extra delay. The first heat exchanger which became full of dust was later replaced with a clean one. The delay after changing the heat exchangers was one minute, which is less than at the start of the trials.

5.3 Data collection

Data from each charge in the converter is stored in a file with 10 second intervals at Avesta Works. The data consists of the mass spectrometer's and IR-spectrometer's measurements, flow rate measured by the V-cone, flow rate of injected gases, etc.

The CO and CO_2 content as well as the V-cone measurements which are used to calculate dC/dt were acquired from these files. For developing the model the decarburization rate just before the carbon sample was needed. Since the blowing is stopped and the converter is tilted during the carbon sample dC/dt just before the blowing is stopped is what is interesting. Because there is a delay in the measurements the values were taken as late as possible after the gas blowing was stopped. This in order to get a value as close as possible to the actual dC/dt before the carbon sample. The V-cone shows reasonable values until 30 seconds after oxygen blowing

is stopped. Therefore the values of CO and CO_2 content and the V-cone measurements were taken 30 seconds after oxygen blowing was stopped.

The flow rate measured by the V-cone fluctuates rather much at the time before the carbon sample. It usually shows values between 85 kNm^3/h and 95 kNm^3/h but the average value over time is usually near 90 kNm^3/h. It would affect the calculations of dC/dt if it happens to be one of the lowest or highest values even though the flow rate as a mean value is stable over time. It would cause a greater spread of the values even though the flow rate as a mean is almost the same between the charges. Therefore, the flow rate used in the calculations was taken as a mean value of the V-cone's measurements for the last minute before the carbon sample.

The values were taken assuming a 1 minute delay. For the charges with a longer delay later values of CO and CO_2 were taken. For example if the delay was 2 minutes the CO and CO_2 values were taken 1 minute later than they would have been if the delay was 1 minute. The flow rate from the V-cone however was always taken in the same way because the delay in gas sampling equipment does not affect the V-cone's measurements.

All the relevant measurements were finally compiled in an Excel file for each steel grade. In Excel it was then possible to plot the carbon content and carbon activity as functions of dC/dt and to find the correlation between them.

5.4 Assumptions and simplifications

The delay for the different charges was varying. It was assumed that the longer delay for some charges did not affect the measured contents, simply displayed it with a longer delay.

The method of measuring the delay was assumed to be accurate, it was however not tested how accurate it is.

It was assumed that the amount of CO and CO_2 from leakage air was negligible.

It is assumed that there is a direct relation between the decarburization rate and the carbon content. There is some relation but it is somewhat loose. It has been suggested in the literature that for each charge there is a direct relation between carbon content and dC/dt but different charges even of the same steel grade may have different correlations [20].

6. Results

6.1 Old sample point

The correlation between carbon content and decarburization rate using the old sample point was estimated for steel grades 316L, S32101, S32205 and 310S. The carbon content was plotted against dC/dt for each grade. The correlation between dC/dt and the carbon content was then given by the equation which Excel calculates using the least square method. Data for the plots regarding carbon content and decarburization rate was acquired from old charge data. The IR-spectrometer was used to measure the CO content in the exhaust gas in all plots. The mass spectrometer was used to measure the CO_2 content in the exhaust gas in all plots except for figure 6.1.4 where the IR-spectrometer was used to measure the CO_2 content. The red square in figure 6.1.5 was disregarded when calculating the equation due to its high deviation, it was however included later when calculating the standard deviation. The standard deviation for the equation in each of the plots is listed in table 6.1.6 in section 6.1.1 and compared to the standard deviation of the equation currently used.

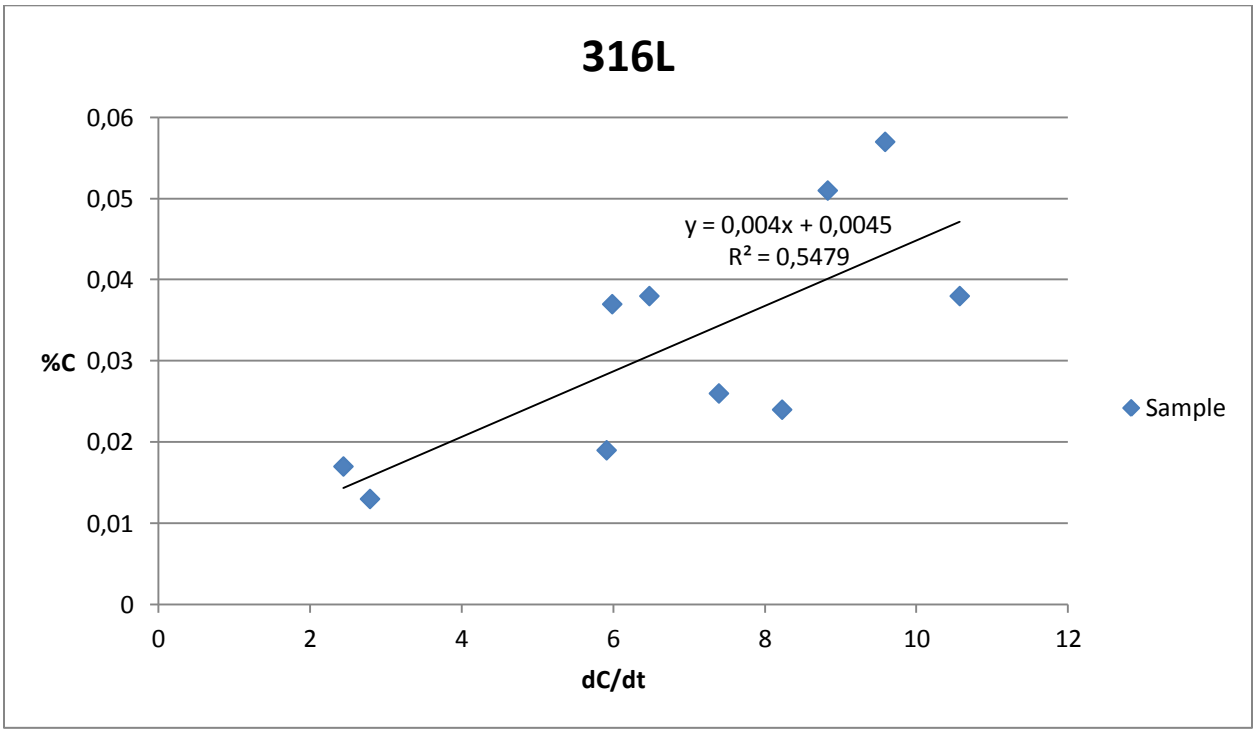

Figure 6.1.1: Decarburization rate plotted versus carbon content for steel grade 316L.

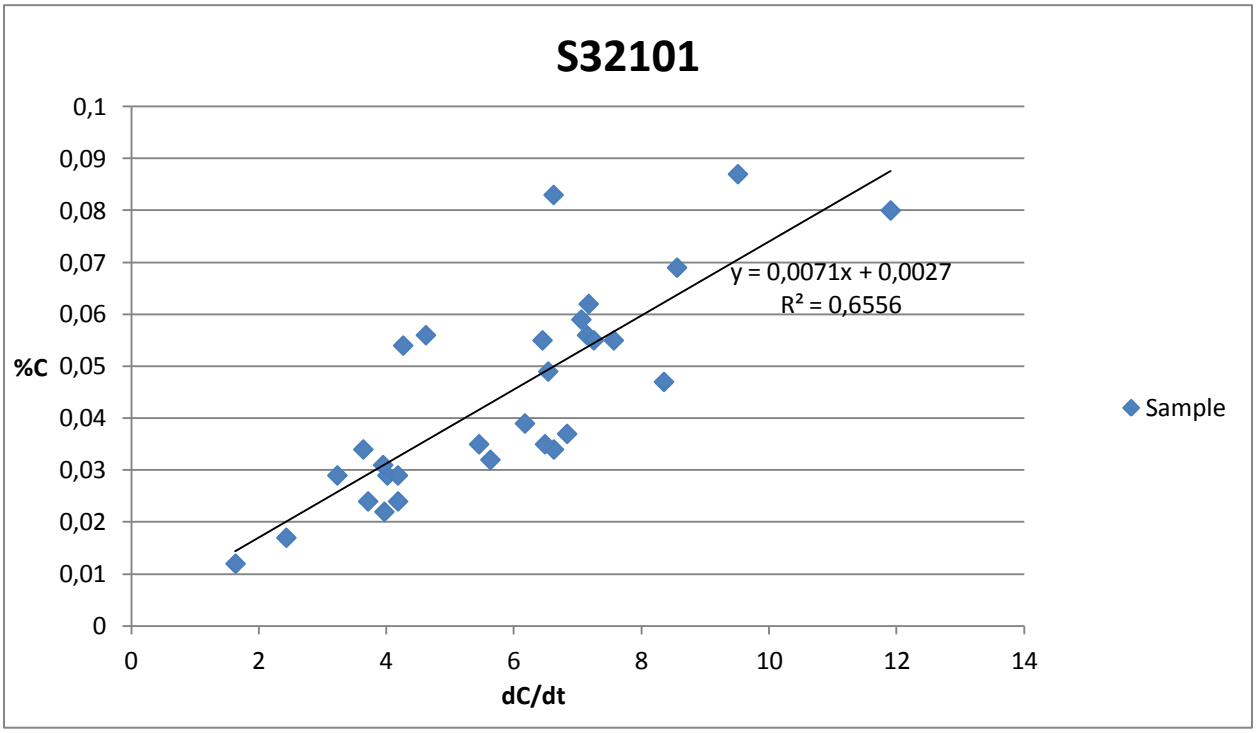

Figure 6.1.2: Decarburization rate plotted versus carbon content for steel grade S32101.

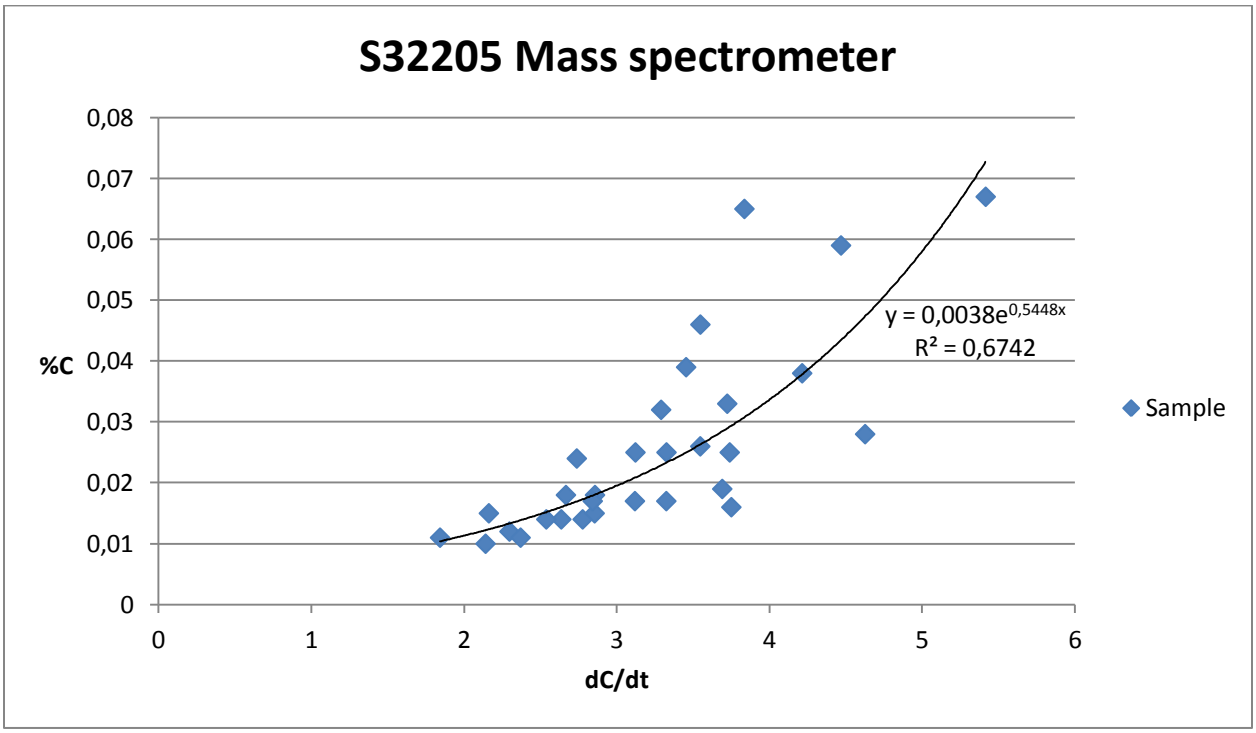

Figure 6.1.3: Decarburization rate plotted versus carbon content for steel grade S32205.

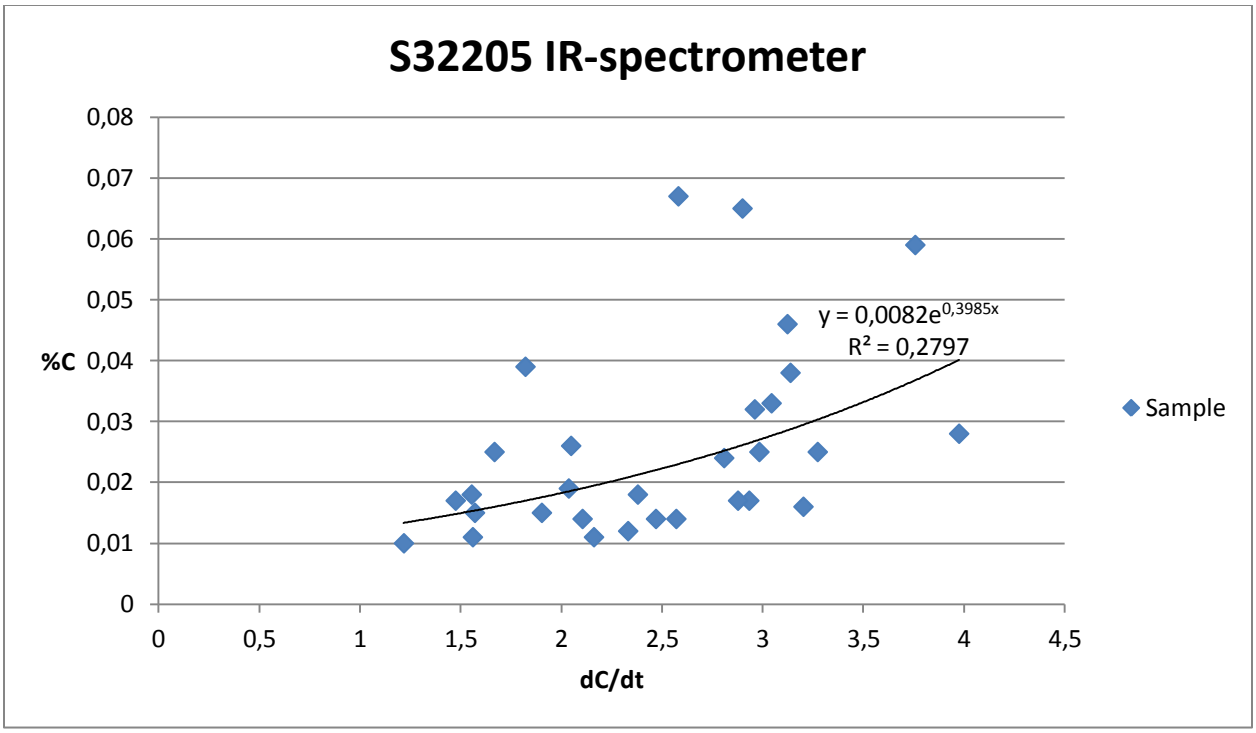

Figure 6.1.4: Decarburization rate plotted versus carbon content for steel grade S32205, CO_2 measured by the IR-spectrometer.

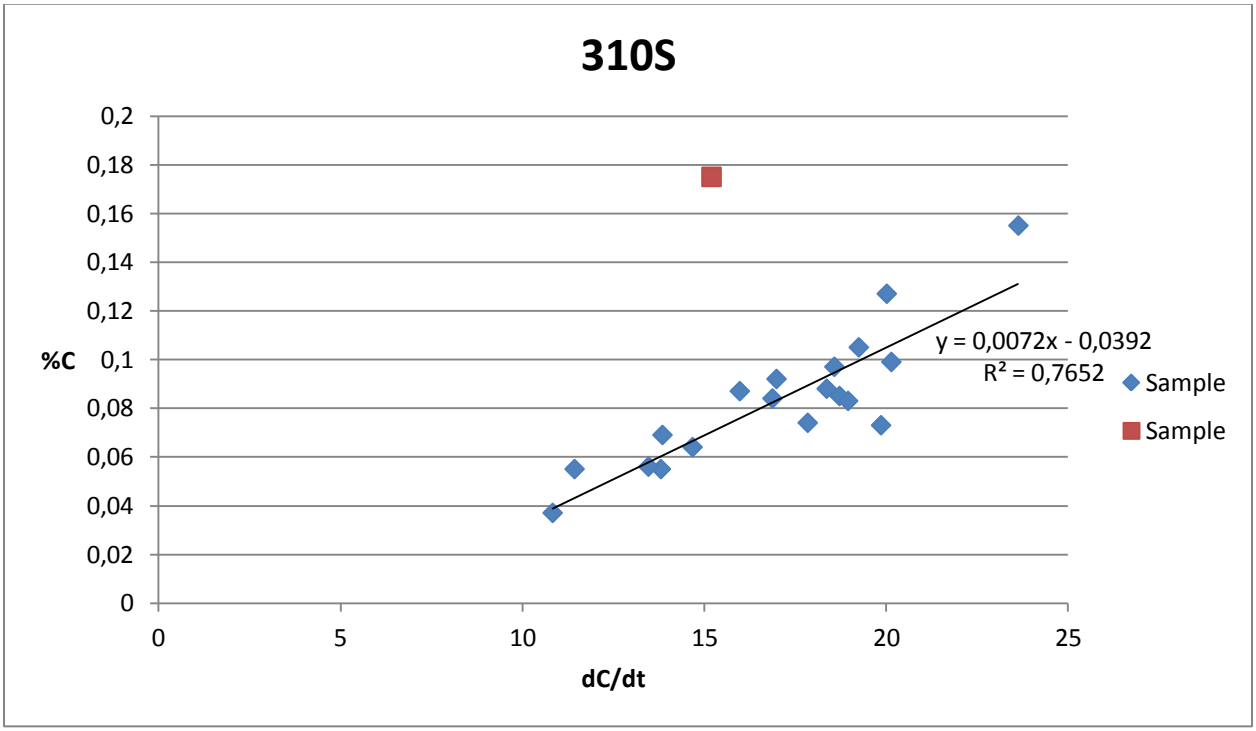

Figure 6.1.5: Steel grade 310S, samples taken at the end of step 3. The red square indicates a sample with high deviation. It was disregarded when calculating the equation but later used when calculating the standard deviation.

6.1.1 Analysis of the old sample point

The standard deviations for the new equations (New standard deviation) acquired from the plots were estimated through Excel's function for standard deviation and compared to the standard deviation of the equations which are currently used (Current standard deviation). The results are listed in the table 6.1.6.

Table 6.1.6: Table displaying the standard deviations when using the equations acquired from the plots compared to the equation which is currently used in the production.

Steel grade (ASTM)	New standard deviation	Current standard deviation
316L	0,00987	0,0106
S32101	0,0115	0,0120
S32205	0,0100	0,0110
S32205 (IR)	0,0140	0,0110
310S	0,0273	0,0272

6.2 New sample point

The correlation between carbon content and decarburization rate using the new sample point was calculated for steel grades 304L, 316L, S32101, S32205 and S30815. The correlation between activity and dC/dt was also plotted and calculated using measurements from the new sample point. In addition dC/dt was measured in two ways. The first was to measure both CO and CO_2 content in the off-gas with the IR-spectrometer, however it works only at CO_2 contents below 1%. The second is to measure the CO with the IR-spectrometer and the CO_2 content with the mass spectrometer. The standard deviations of the new equations were then estimated through Excel's function for standard deviation and are listed in table 6.2.7.1 in section 6.2.7. For the plots with dC/dt measured only by the IR-spectrometer an additional line was drawn. This line represents the upper boundary of the samples, disregarding 20% of the samples with the highest positive deviation. It was drawn so it will cut both the x- and y-axis at (0,0).

6.2.1 304L

The plots in section 6.2.1 represent samples of steel grade 304L where the carbon content has been plotted against dC/dt in figure 6.2.1.1-6.2.1.3 and the carbon activity against dC/dt in 6.2.1.4. In figure 6.2.1.1 the CO_2 was measured by the IR-spectrometer and there are two equations. The upper line represents the upper boundary for 80% of the samples. The lower line was calculated by Excel using the least square method. The red square represents a sample with high deviation and was disregarded when calculating the lower equation but it is considered later when calculating the standard deviation. Figure 6.2.1.2 represents the same samples as figure 6.2.1.1 but with the CO_2 measured by the mass spectrometer. Figure 6.2.1.3 represents all of the samples taken during this master thesis. The samples where the CO_2 content was over 1% are also included in the plot. Figure 6.2.1.4 represents the same samples

as in figure 6.2.1.1 with the CO_2 content measured by the IR-spectrometer, but with the carbon activity instead of the carbon content on the y-axis.

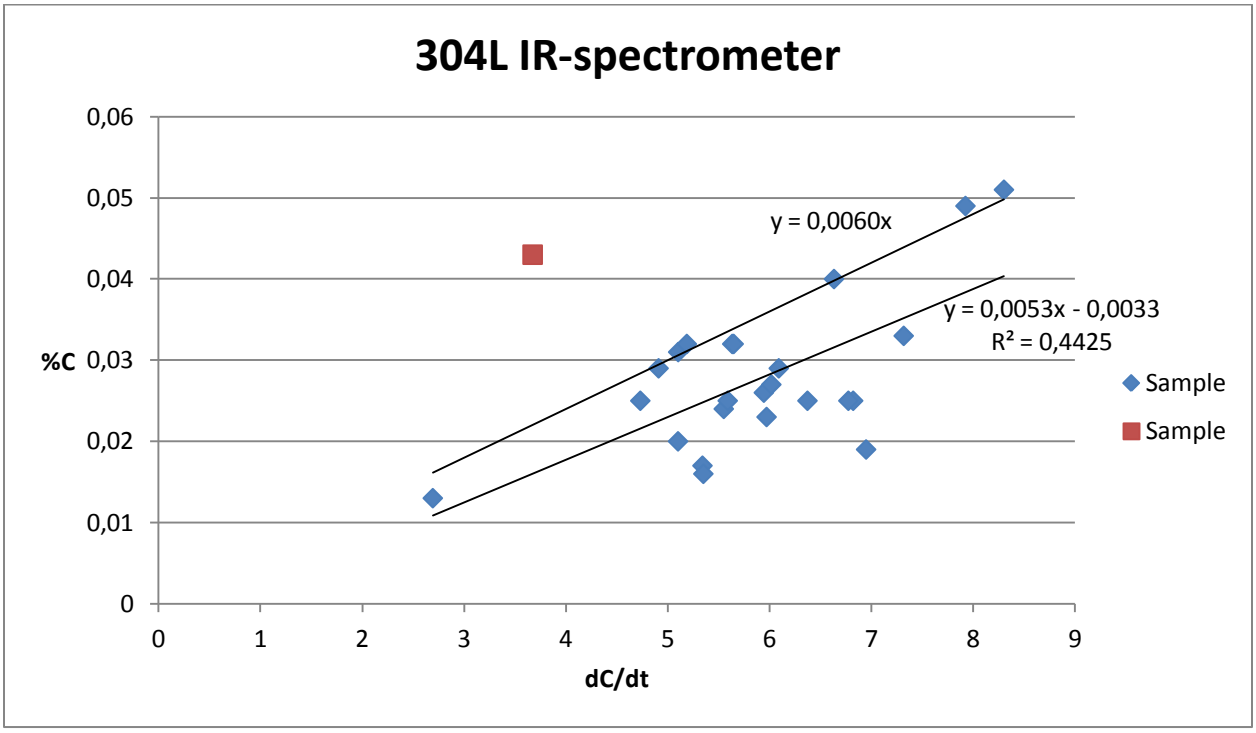

Figure 6.2.1.1: Steel grade 304L, CO_2 measured by the IR-spectrometer.

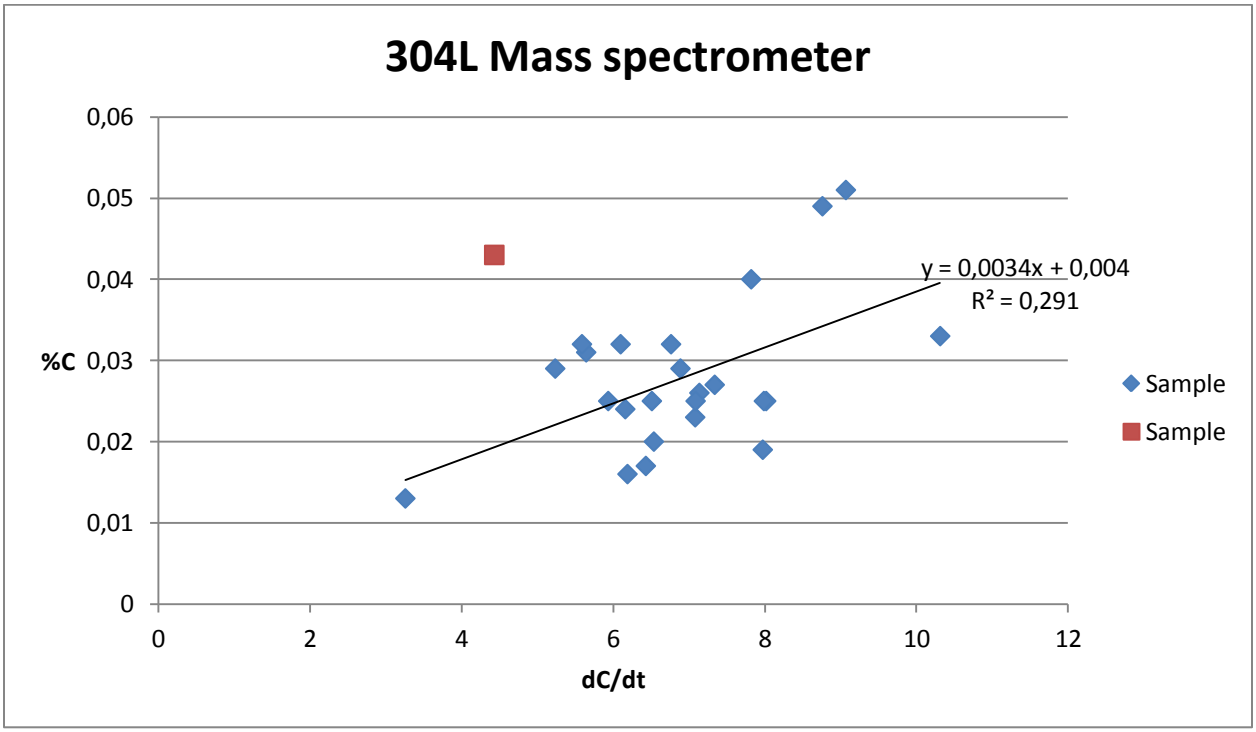

Figure 6.2.1.2: Steel grade 304L, CO_2 measured by the mass spectrometer. Same samples as in 6.2.1.1.

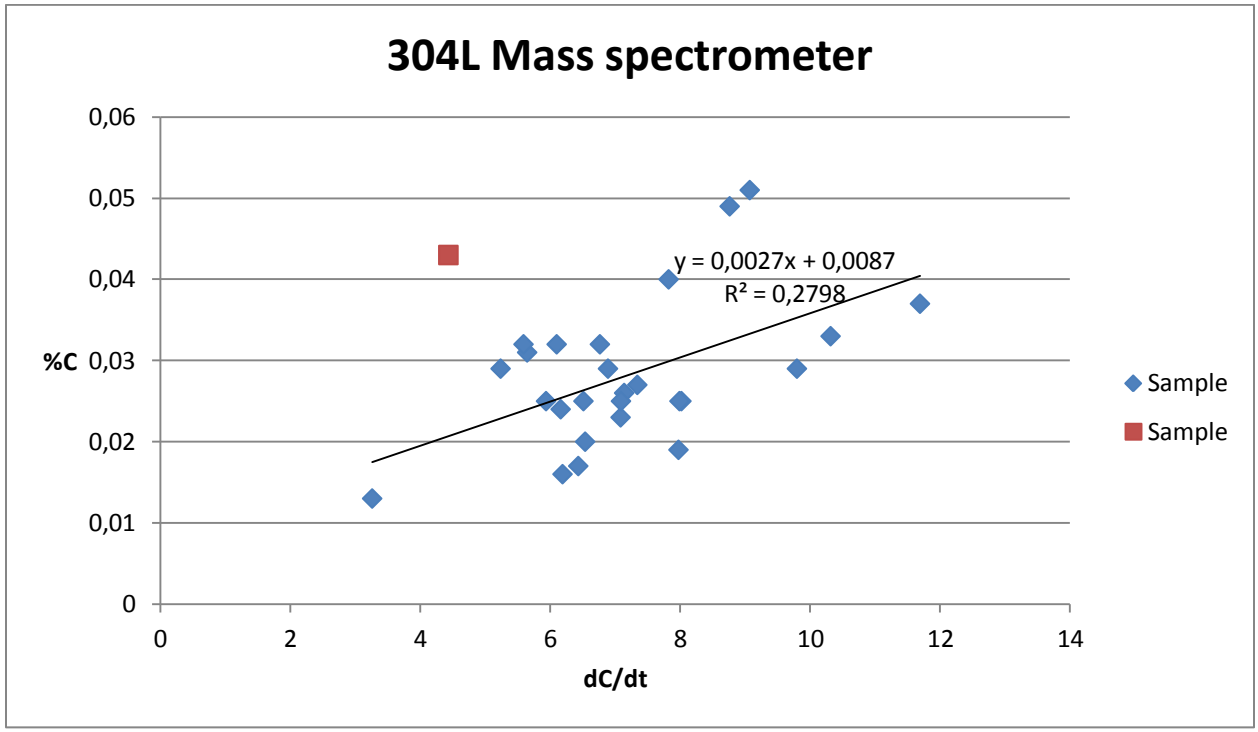

Figure 6.2.1.3: Steel grade 304L, CO_2 measured by the mass spectrometer. Including all acquired samples.

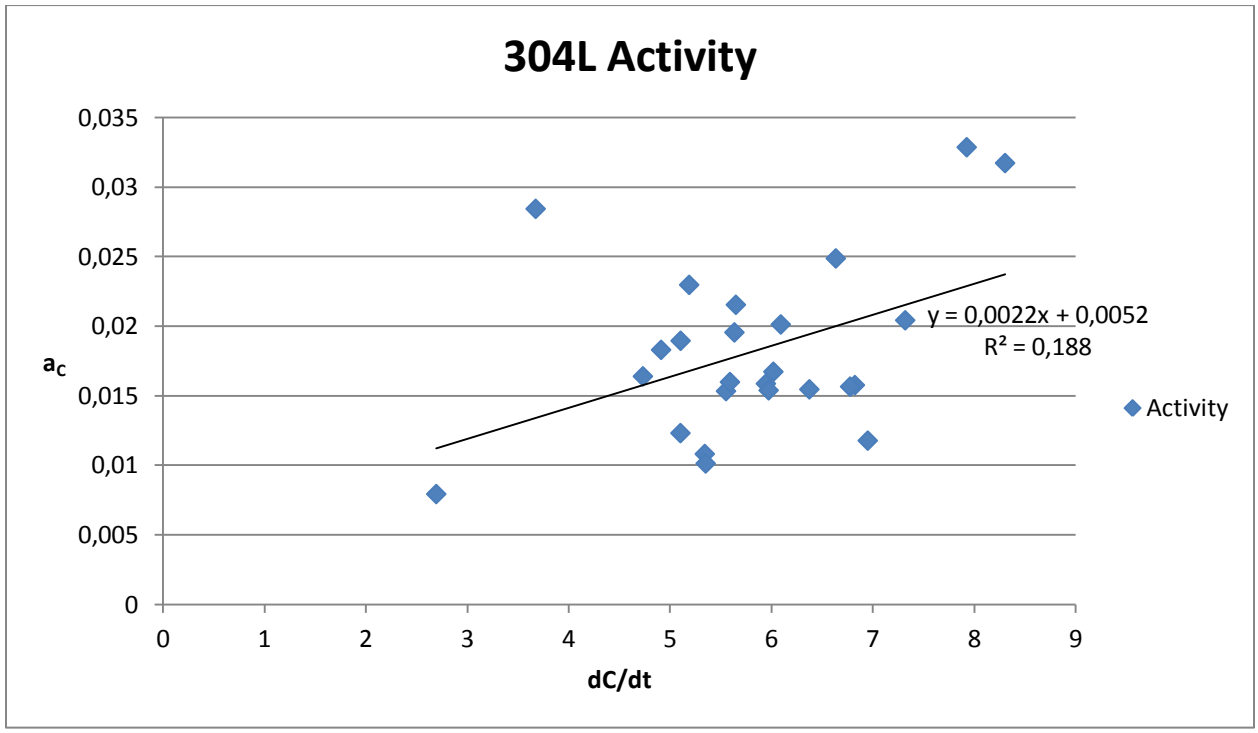

Figure 6.2.1.4: Steel grade 304L, CO_2 measured by the IR-spectrometer. Linear regression between dC/dt and carbon activity.

6.2.2 316L

The plots in section 6.2.2 represent samples of steel grade 316L, where the carbon content has been plotted against dC/dt in figure 6.2.2.1-6.2.2.3 and the carbon activity against dC/dt in 6.2.2.4. In figure 6.2.2.1 the CO_2 was measured by the IR-spectrometer and there are two equations. The upper line represents the upper boundary for 80% of the samples. The lower line was calculated by Excel using the least square method. Figure 6.2.2.2 represents the same samples as figure 6.2.2.1 but with the CO_2 measured by the mass spectrometer. Figure 6.2.2.3 represents all of the samples taken during this master thesis. The samples where the CO_2 content was over 1% are also included in the plot. Figure 6.2.2.4 represents the same samples as in figure 6.2.2.1 with the CO_2 content measured by the IR-spectrometer, but with the carbon activity instead of the carbon content on the y-axis.

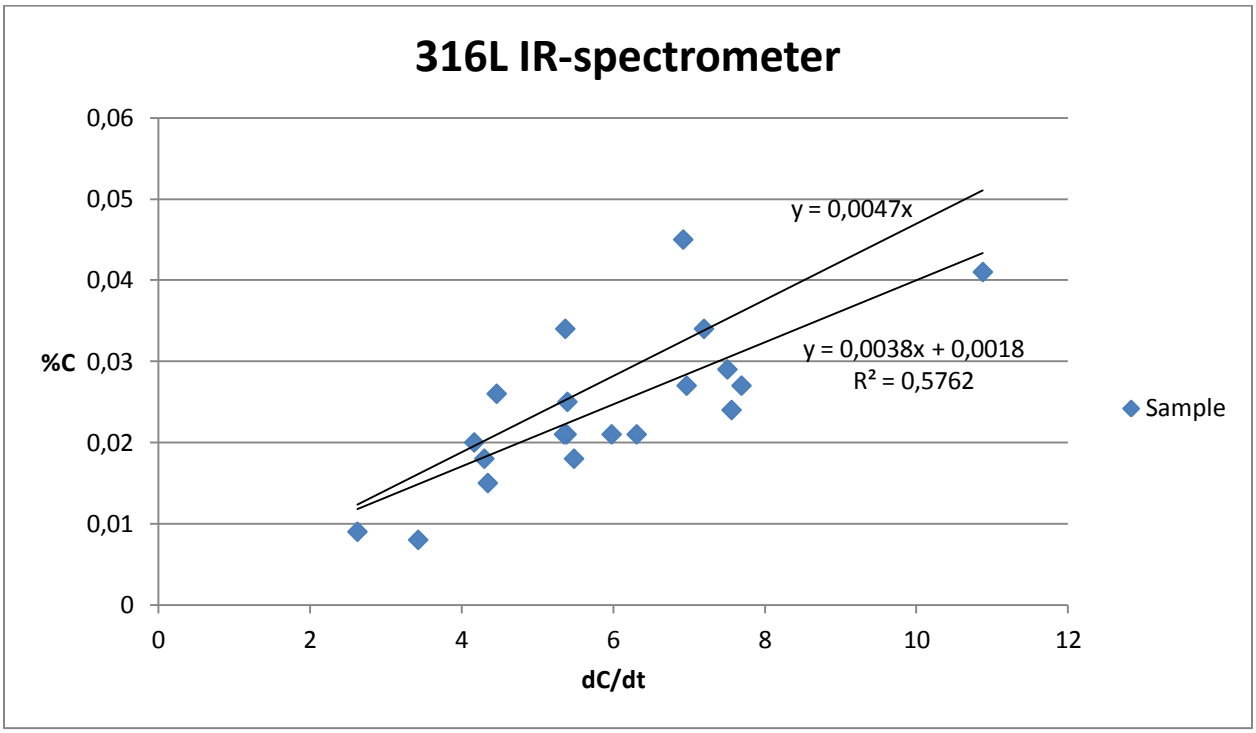

Figure 6.2.2.1: Steel grade 316L, CO_2 measured by the IR-spectrometer.

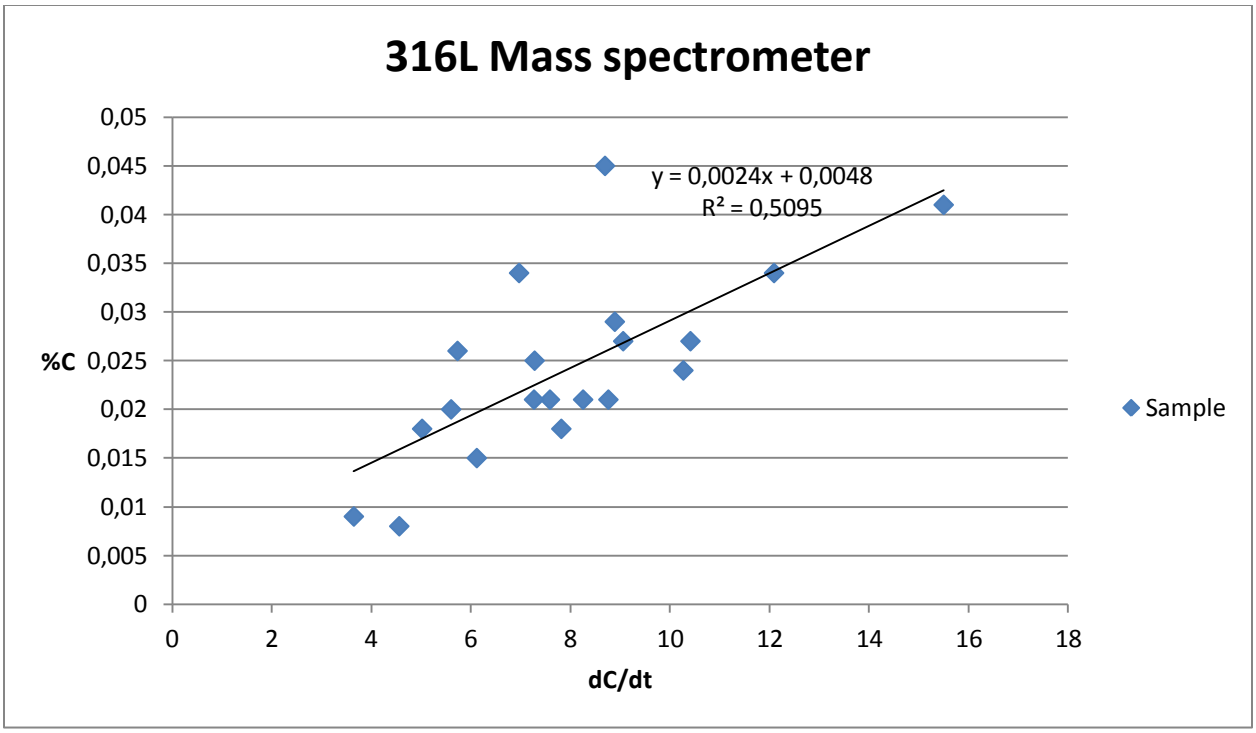

Figure 6.2.2.2: Steel grade 316L, CO_2 measured by the mass spectrometer. Same samples as in 6.2.2.1.

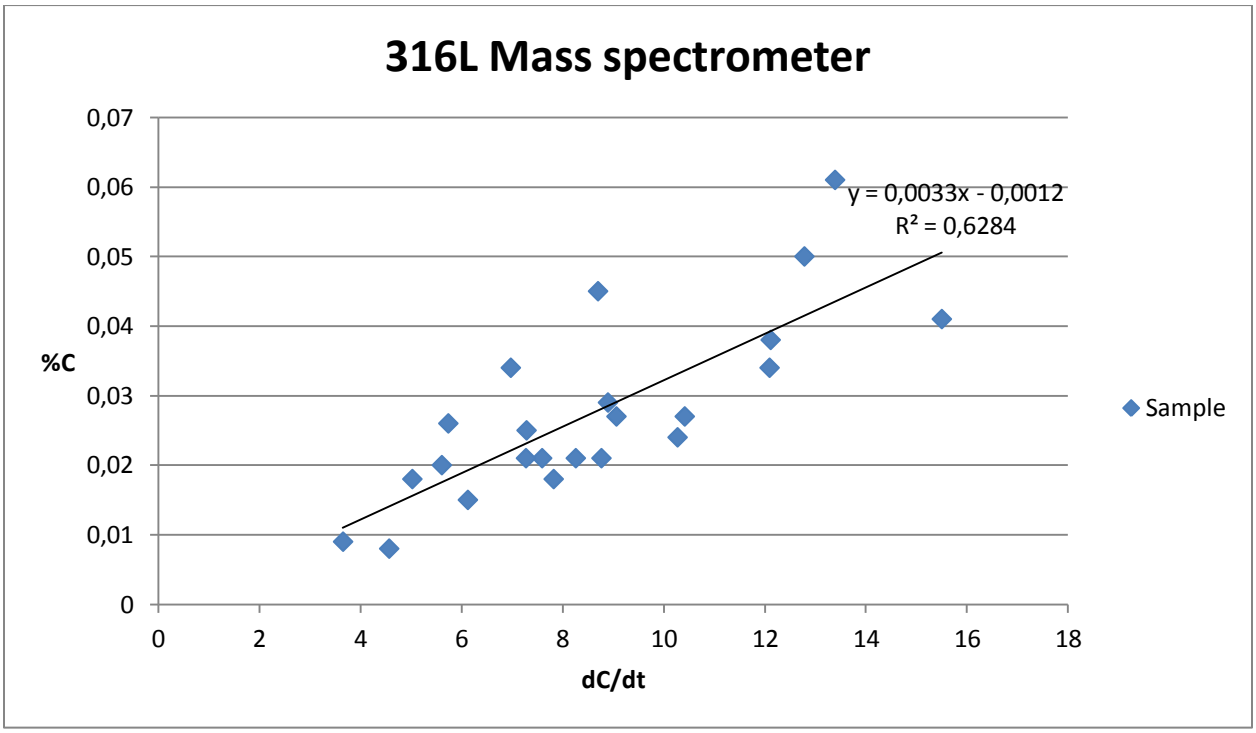

Figure 6.2.2.3: Steel grade 316L, CO_2 measured by the mass spectrometer. Including all acquired samples.

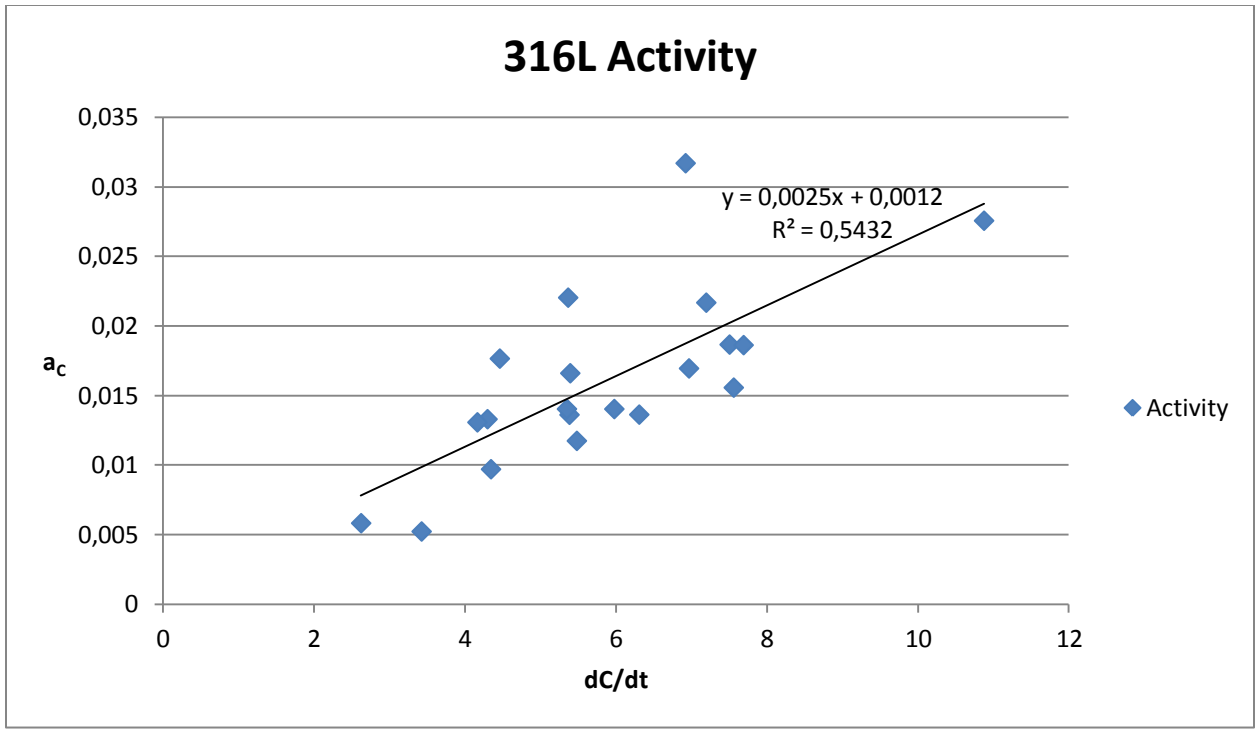

Figure 6.2.2.4: Steel grade 316L, CO_2 measured by the IR-spectrometer. Linear regression between dC/dt and carbon activity.

6.2.3 S32101

The plots in section 6.2.3 represent samples of steel grade S32101, where the carbon content has been plotted against dC/dt in figure 6.2.3.1-6.2.3.3 and the carbon activity against dC/dt in 6.2.3.4. In figure 6.2.3.1 the CO_2 was measured by the IR-spectrometer and there are two equations. The upper line represents the upper boundary for 80% of the samples. The lower line was calculated by Excel using the least square method. Figure 6.2.3.2 represents the same samples as figure 6.2.3.1 but with the CO_2 measured by the mass spectrometer. Figure 6.2.3.3 represents all of the samples taken during this master thesis. The samples where the CO_2 content was over 1% are also included in the plot. Figure 6.2.3.4 represents the same samples as in figure 6.2.3.1 with the CO_2 content measured by the IR-spectrometer, but with the carbon activity instead of the carbon content on the y-axis.

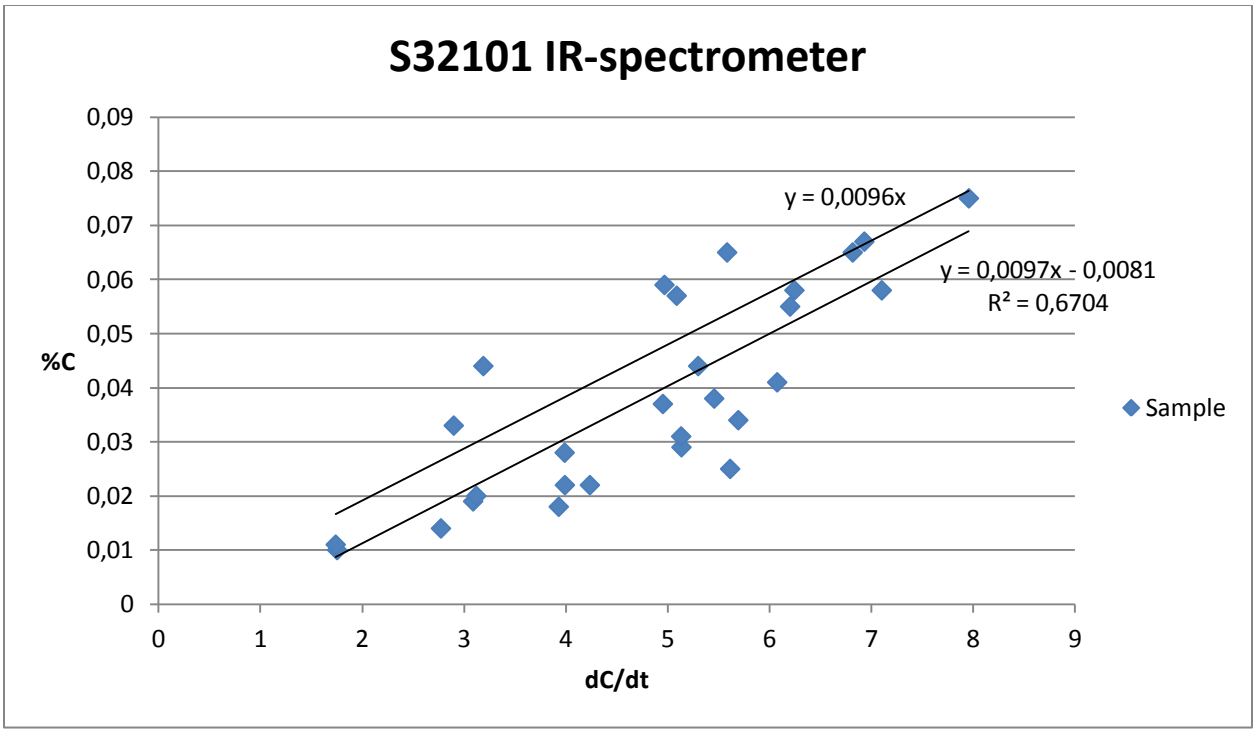

Figure 6.2.3.1: Steel grade S32101, CO_2 measured by the IR-spectrometer.

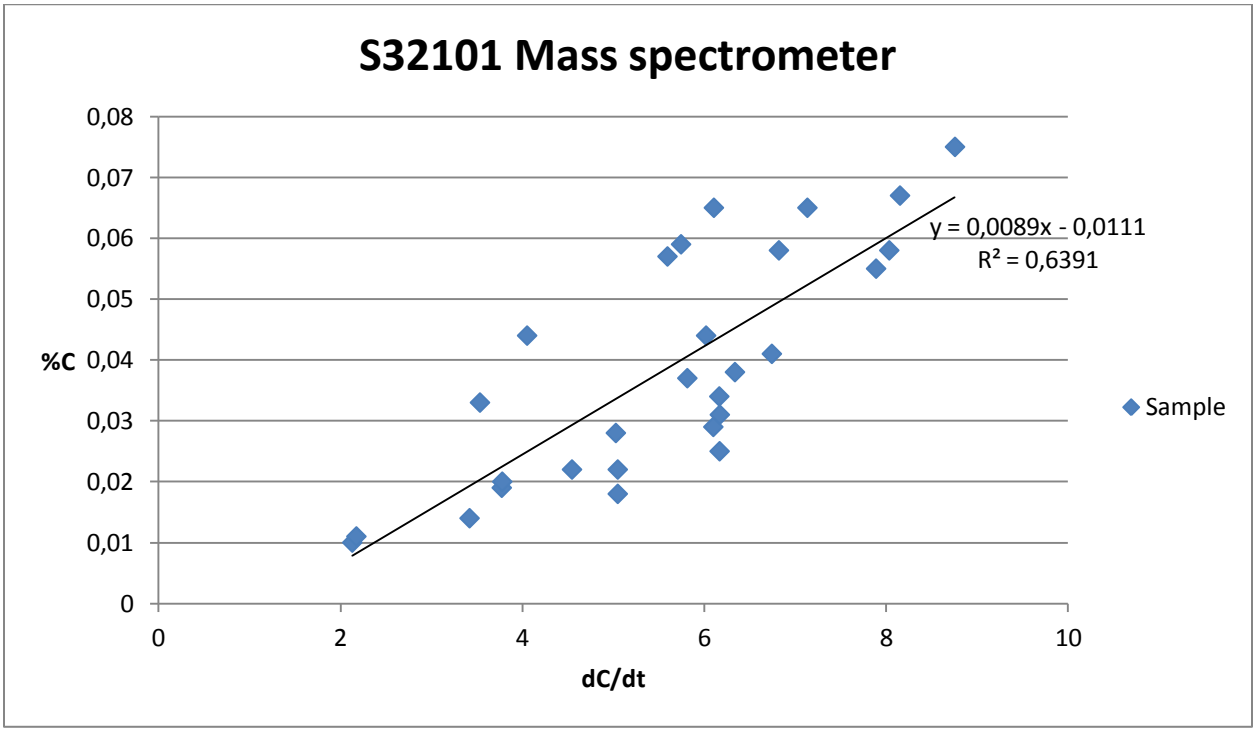

Figure 6.2.3.2: Steel grade S32101, CO_2 measured by the mass spectrometer. Same samples as in 6.2.3.1.

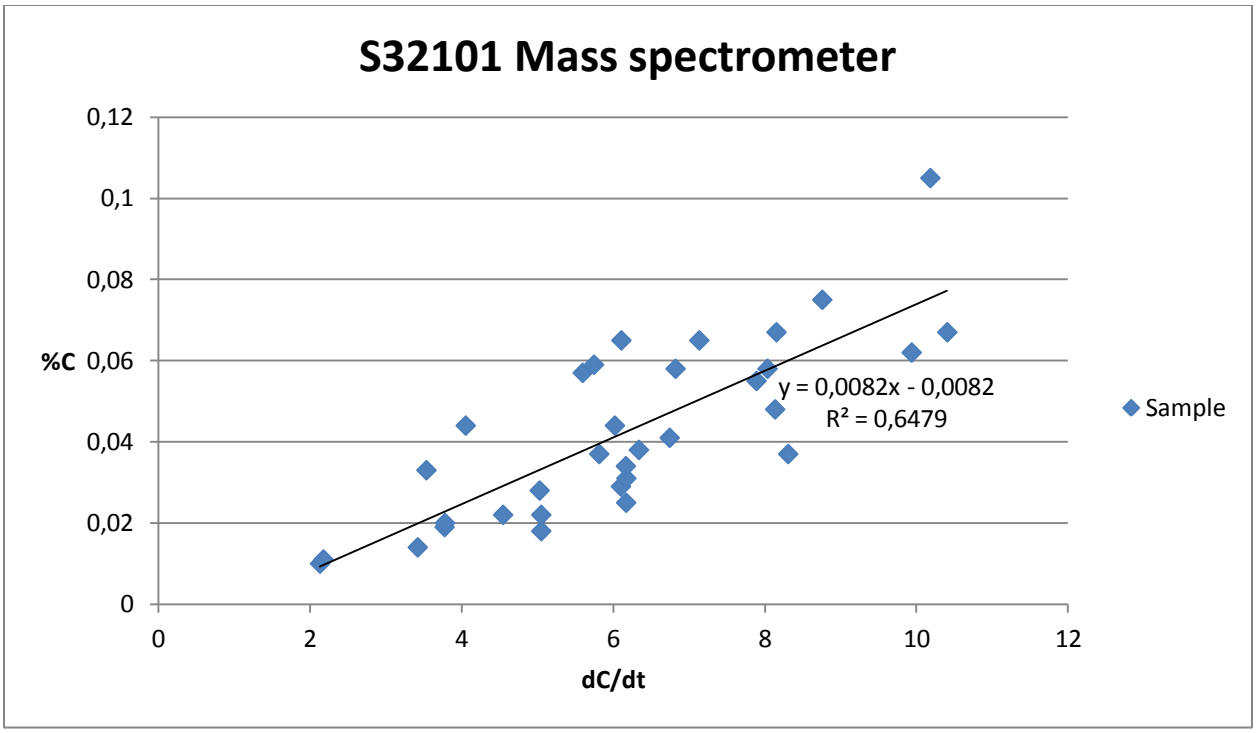

Figure 6.2.3.3: Steel grade S32101, CO_2 measured by the mass spectrometer. Including all acquires samples.

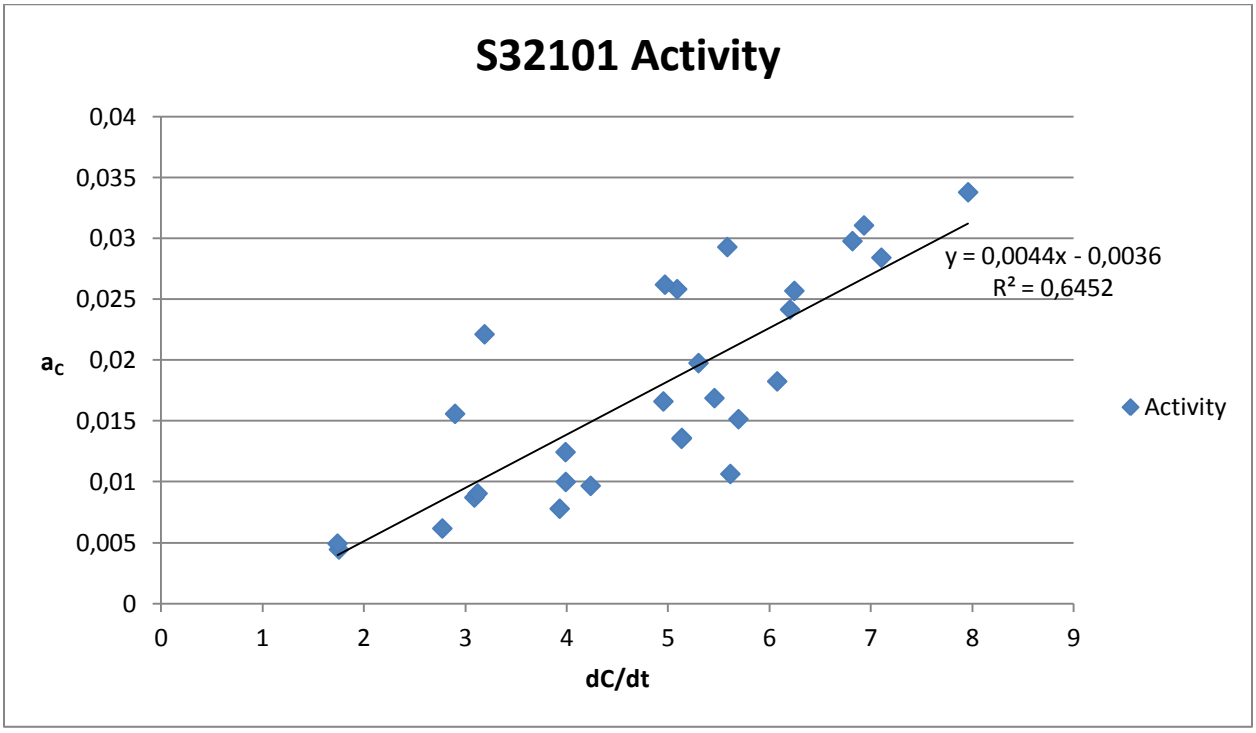

Figure 6.2.3.4: Steel grade S32101, CO_2 measured by the IR-spectrometer. Linear regression between dC/dt and carbon activity.

6.2.4 S32205

The plots in section 6.2.4 represent samples of steel grade S32205, where the carbon content has been plotted against dC/dt in figure 6.2.4.1-6.2.4.4 and the carbon activity against dC/dt in 6.2.4.5. In figure 6.2.4.1 the CO_2 was measured by the IR-spectrometer and there are two equations. The upper line represents the upper boundary for 80% of the samples. The lower line was calculated by Excel using the least square method. Figure 6.2.4.2 represents the same samples as in figure 6.2.4.1 with the CO_2 content measured by the IR-spectrometer. The equation is however an exponential equation. Steel grade S32205 was the only steel grade for which an exponential equation yielded a lower standard deviation than a linear equation. Figure 6.2.4.3 represents the same samples as figure 6.2.4.1 but with the CO_2 measured by the mass spectrometer. Figure 6.2.4.4 represents all of the samples taken during this master thesis. The samples where the CO_2 content was over 1% are also included in the plot. Figure 6.2.4.5 represents the same samples as in figure 6.2.4.1 with the CO_2 content measured by the IR-spectrometer, but with the carbon activity instead of the carbon content on the y-axis.

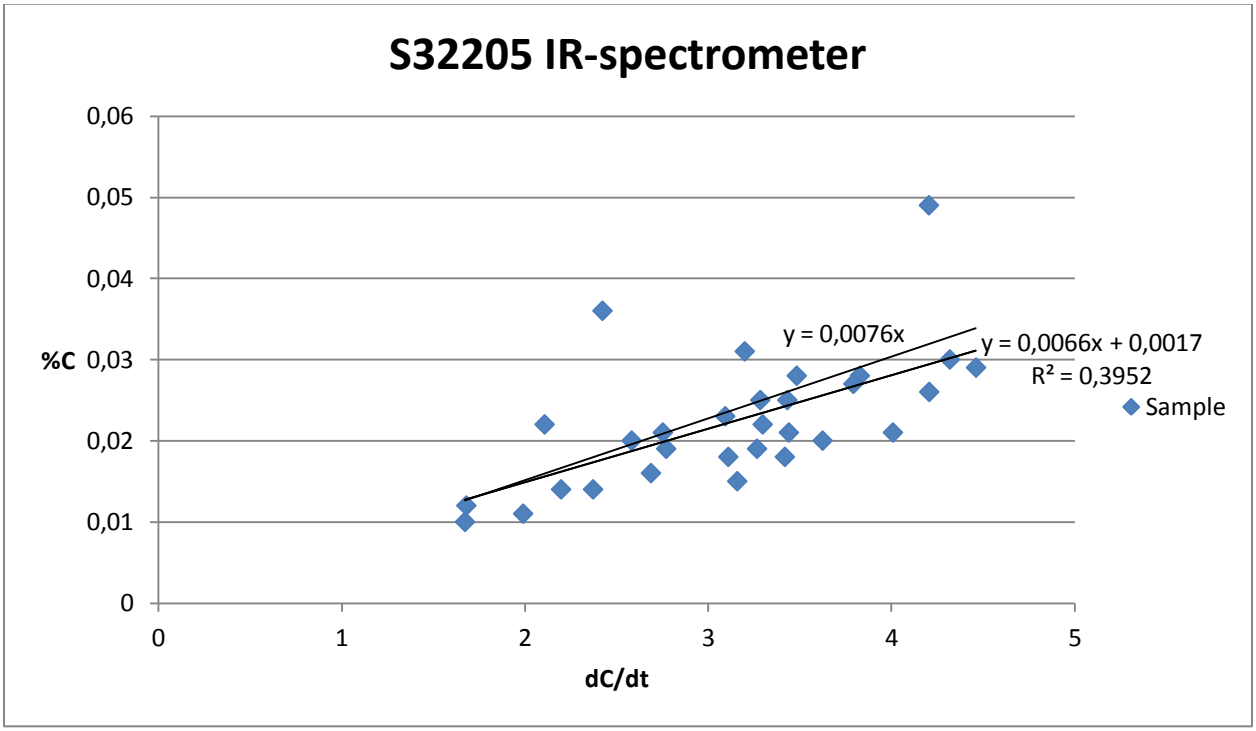

Figure 6.2.4.1: Steel grade S32205, CO_2 measured by the IR-spectrometer.

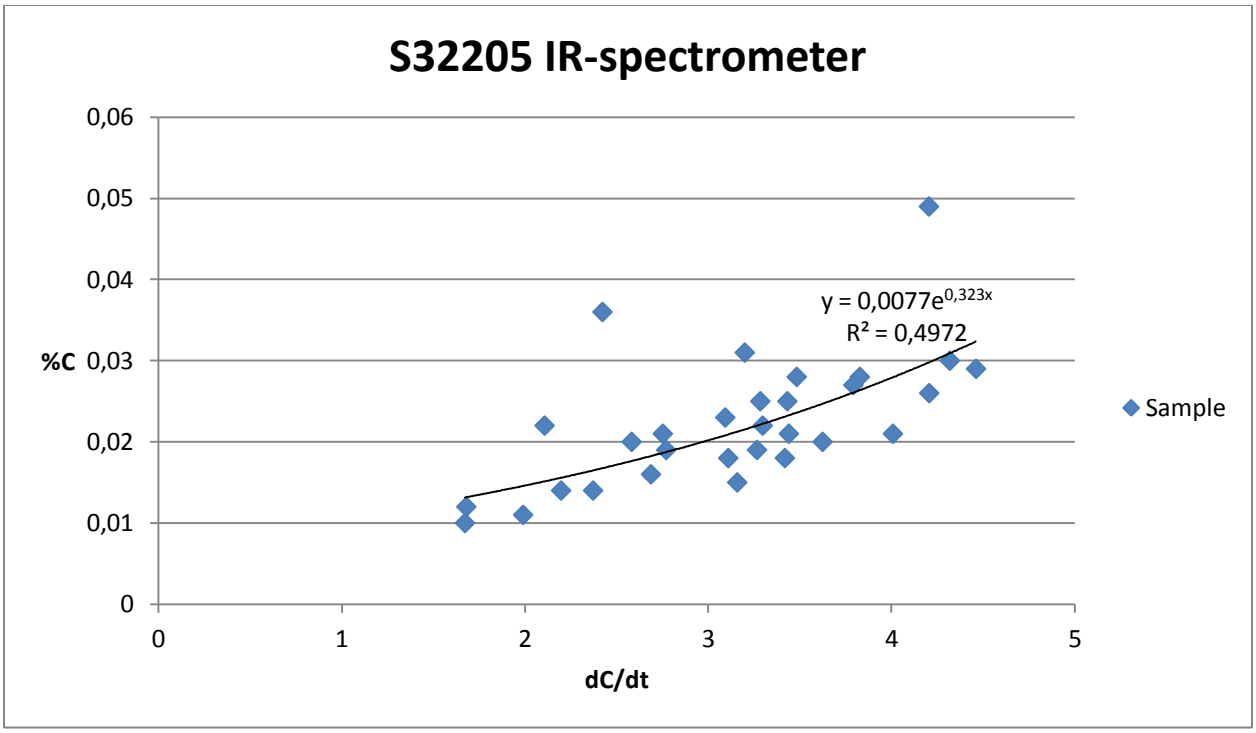

Figure 6.2.4.2: Steel grade S32205, CO_2 measured by the IR-spectrometer. Exponential equation.

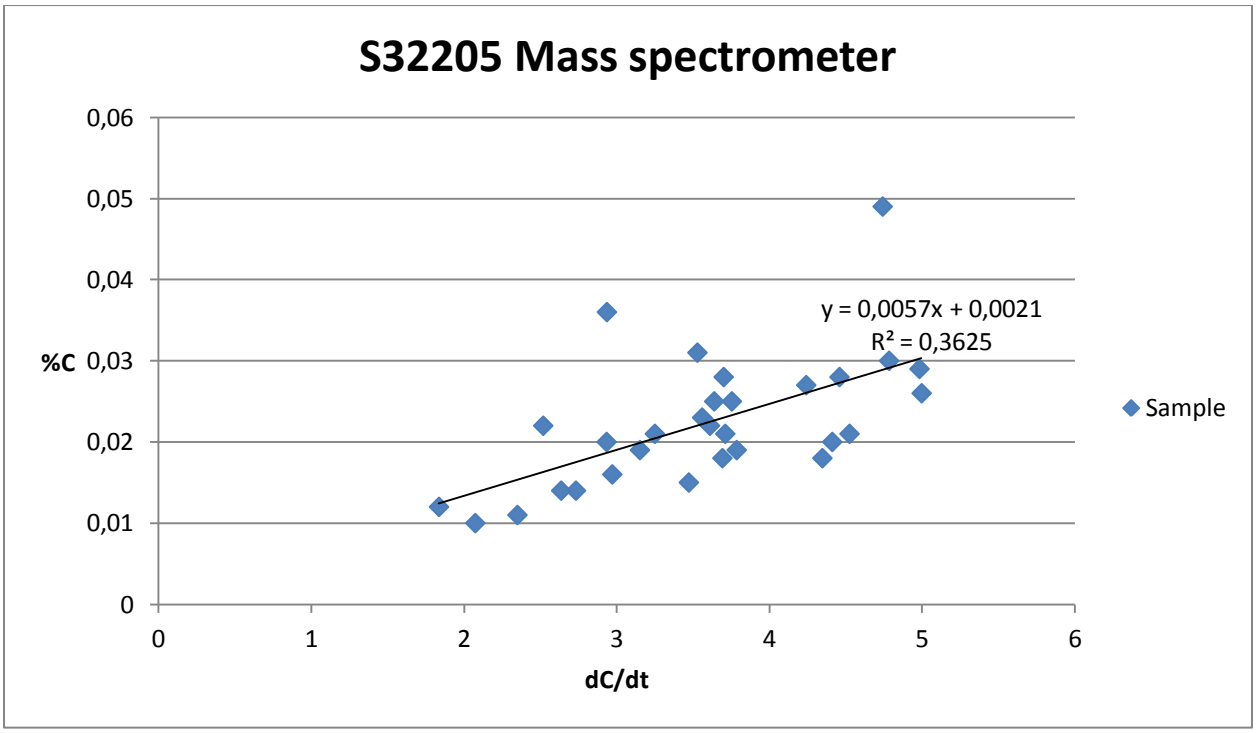

Figure 6.2.4.3: Steel grade S32205, CO_2 measured by the mass spectrometer. Same samples as in 6.2.4.1.

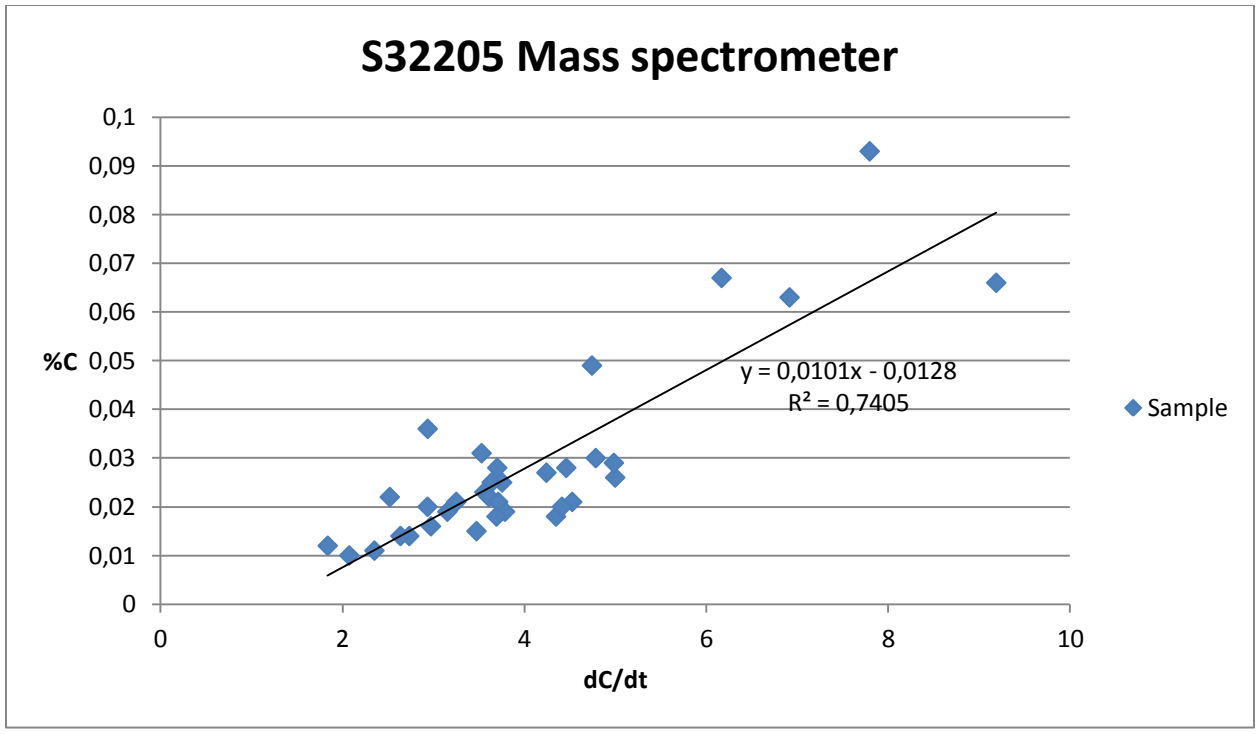

Figure 6.2.4.4: Steel grade S32205, CO_2 measured by the mass spectrometer. All acquired samples included.

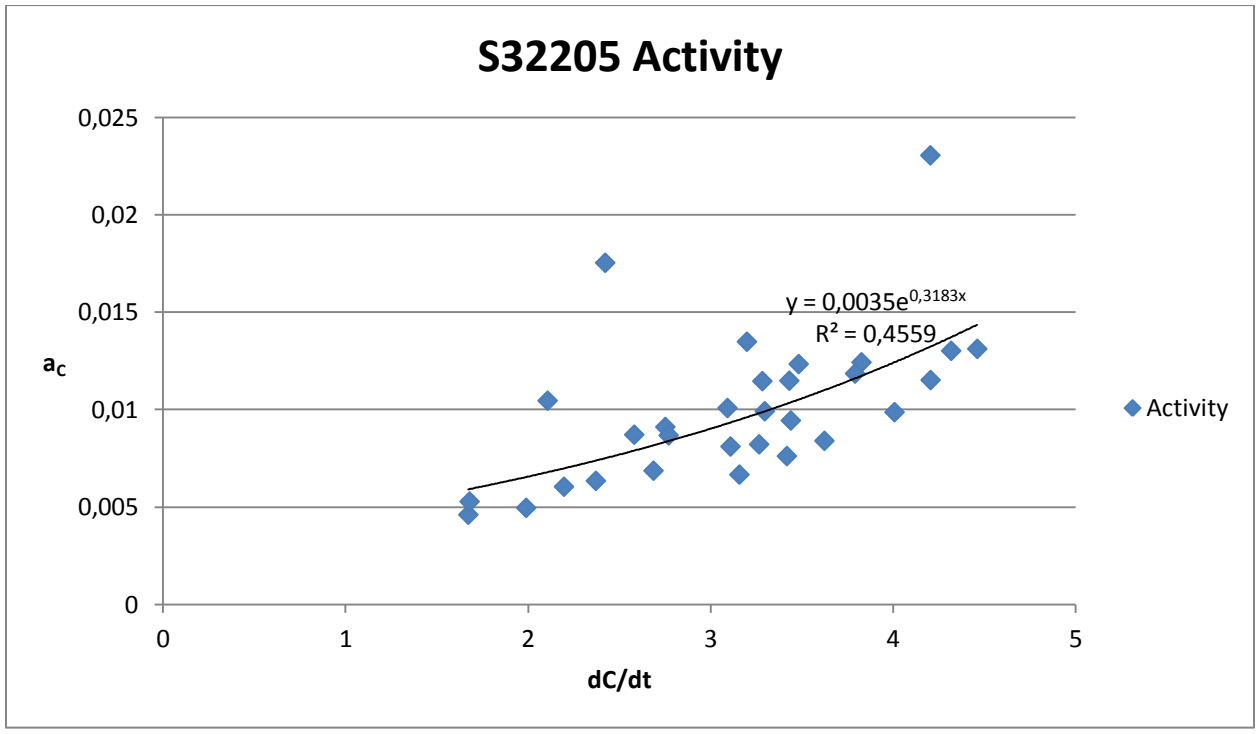

Figure 6.2.4.5: Steel grade S32205, CO_2 measured by the IR-spectrometer. Exponential regression between dC/dt and carbon activity.

6.2.5 S32205 (step 3)

The plots in section 6.2.5 represent samples of steel grade S32205 taken at the end of step 3, where the carbon content and the carbon activity has been plotted against dC/dt. The CO_2 content was measured by the mass spectrometer in both plots. In figure 6.2.5.1 the carbon content is plotted against dC/dt. In figure 6.2.5.2 the carbon activity is plotted against dC/dt.

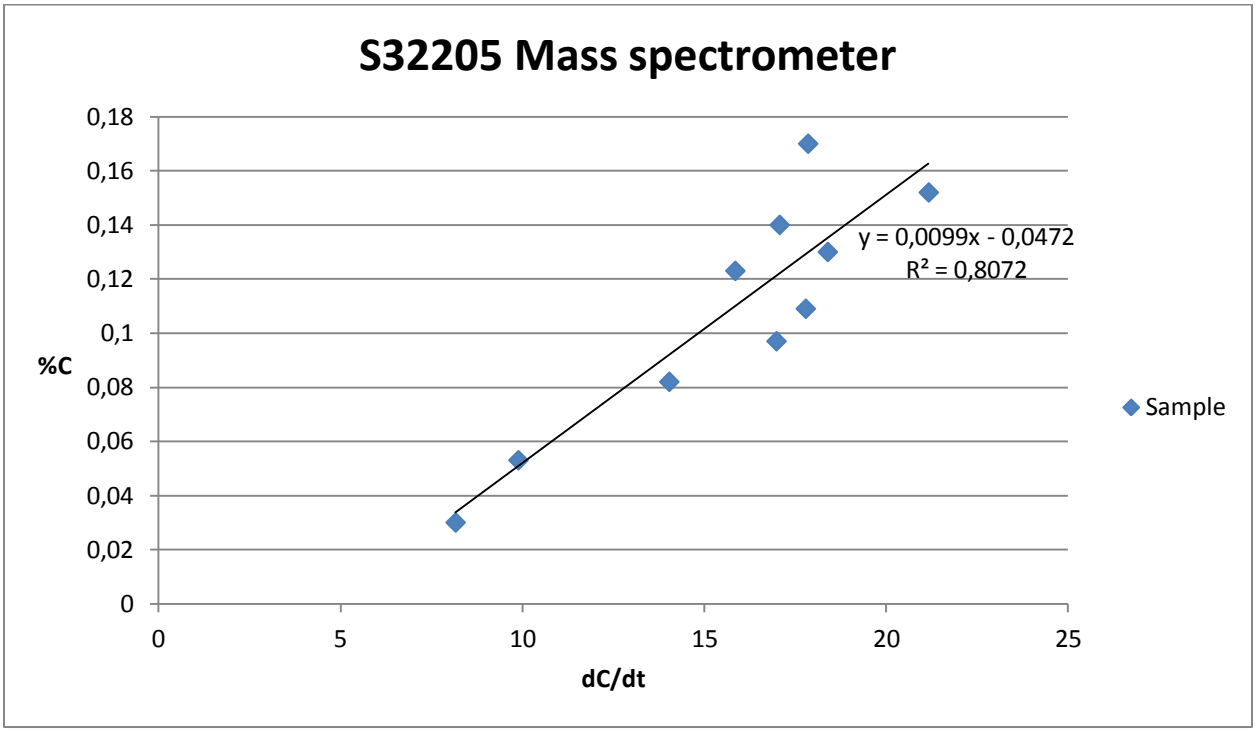

Figure 6.2.5.1: Steel grade S32205, CO_2 measured by the mass spectrometer. Samples taken at the end of step 3.

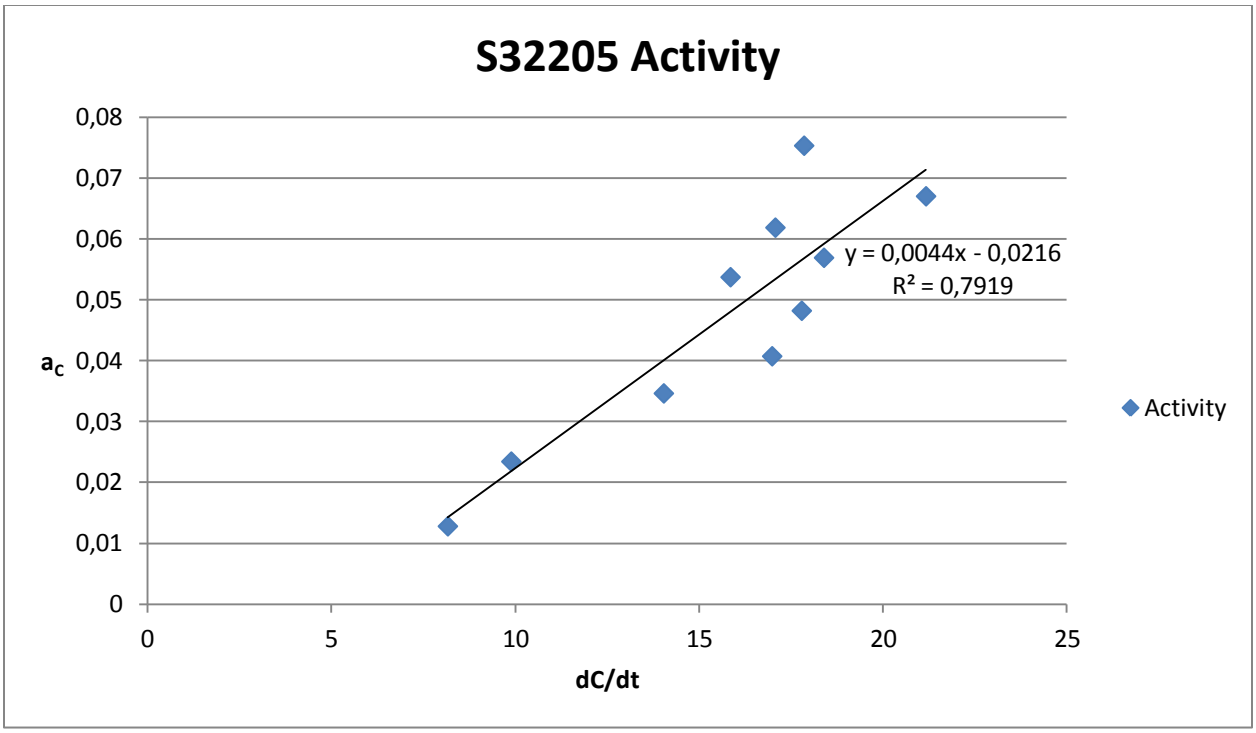

Figure 6.2.5.2: Steel grade S32205, CO_2 measured by the mass spectrometer. Samples taken at the end of step 3. Linear regression between dC/dt and carbon activity.

6.2.6 S30815

The plots in section 6.2.6 represent samples of steel grade S30815 taken at the end of step 3, where the carbon content and the carbon activity has been plotted against dC/dt. The CO_2 content was measured by the mass spectrometer in both plots. In figure 6.2.6.1 the carbon content is plotted against dC/dt. In figure 6.2.6.2 the carbon activity is plotted against dC/dt.

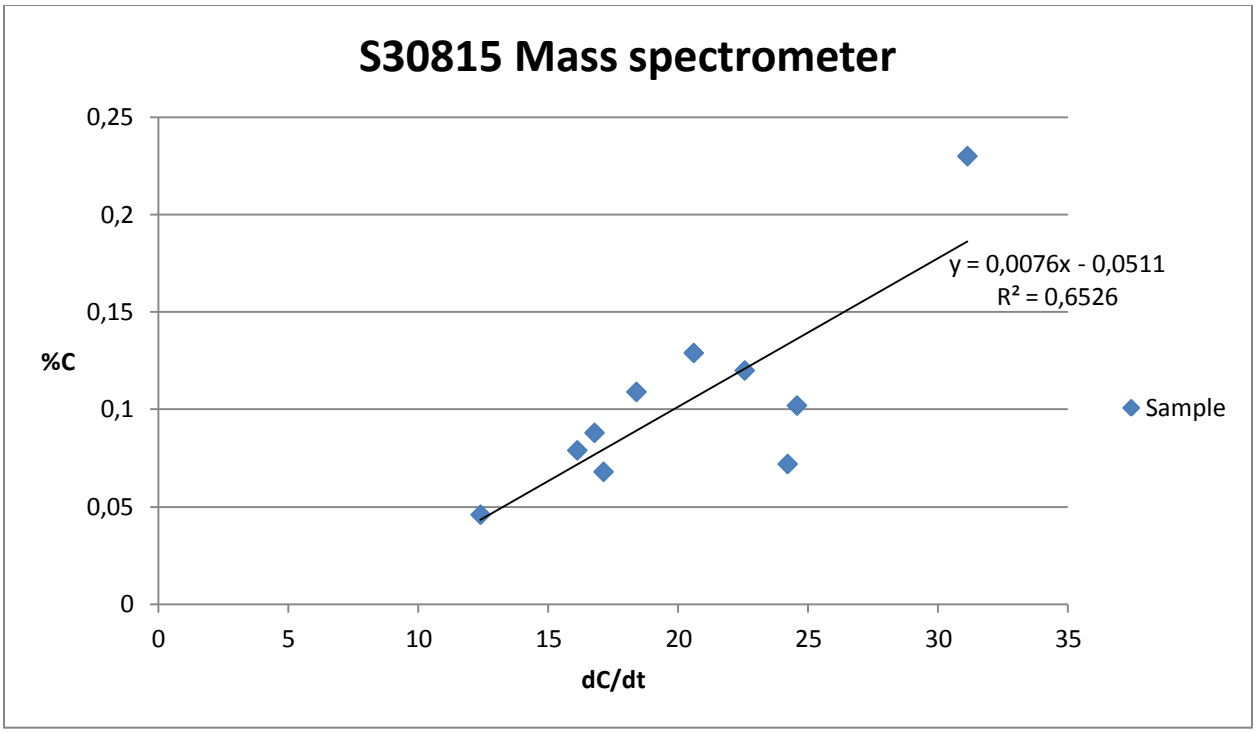

Figure 6.2.6.1: Steel grade S30815, CO_2 measured by the mass spectrometer. Samples taken at the end of step 3.

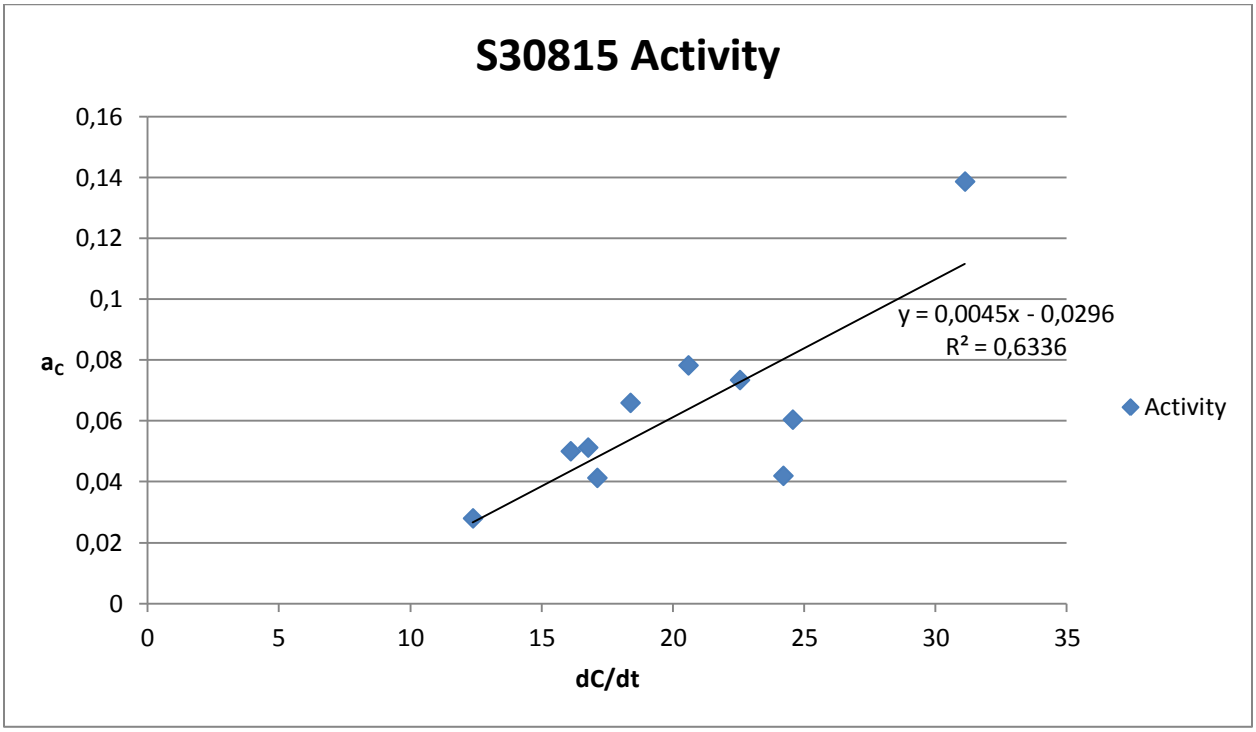

Figure 6.2.6.2: Steel grade S30815, CO_2 measured by the mass spectrometer. Samples taken at the end of step 3. Linear regression between dC/dt and carbon activity.

6.2.7 Analysis of the new equations

The kind of regression which turned out to give the smallest standard deviation was the linear regression. However, for one steel grade S32205 an exponential regression gave a slightly lower standard deviation 0,00626 %C compared to 0,00627 %C for the linear regression. The standard deviations for some of the different equations are listed in table 6.2.7.1. It includes samples with measurements made by the IR-spectrometer. The same samples for which measurements were made by the IR-spectrometer but with measurements made by the mass spectrometer instead. All analyzed samples including some samples with CO_2 contents over 1% measured by the mass spectrometer and the standard deviation when using the activity. Standard deviations for S32205 are given for the exponential equations in IR-spectrometer and activity.

Table 6.2.7.1: Steel grades which were included in the study of the new sample point. Shows the standard deviations of each steel grade when using the equations acquired in the plots in section 6.2.1-6.2.6.

Steel grade (ASTM)	IR-spectrometer	Mass spectrometer, CO_2 below 1%	Mass spectrometer, all samples	Activity	Upper boundary
304L	0,00860	0,00764	0,00860	0,00875	0,00732
316L	0,00609	0,00655	0,00782	0,00639	0,00630
S32101	0,0109	0,0114	0,0129	0,0115	0,0109
S32205	0,00626	0,00644	0,00941	0,00664	0,00632
S32205 (step 3)			0,0193	0,0206	
S30815			0,0300	0,0315	

6.2.8 General carbon prediction formula

With the upper boundary equations it was possible to derive an expression of how the constant in the equations depends on the steel composition. For steel grades 304L, 316L, S32101 and S32205 the average steel composition during the time of the carbon sample was calculated. Only Cr, Ni, Mn and Mo which are the four most significant alloying elements were considered. Equations of how the constant in the upper boundary equation depends on the composition could then be formed. Since it was done for four steel grades and for four different alloying elements there were four equations and four unknown variables. The average contents of Cr, Ni, Mn and Mo as well as the constant k from the upper boundary equation are listed in table 6.2.8.1.

Table 6.2.8.1: Average Cr, Ni, Mn and Mo content during the time of the carbon sample and the constant k in the upper boundary equation for steel grades 304L, 316L, S32205 and S32101.

Steel grade (ASTM)	Cr	Ni	Mn	Mo	k
304L	16,48	8,45	0,64	0,49	0,006
316L	15,24	10,55	0,63	2,14	0,0047
S32205	20,39	5,37	0,44	3,06	0,0076
S32101	20,20	1,52	0,90	0,27	0,0096

The equations were arranged in matrices with one variable assigned to each alloying element. The matrices were solved in Matlab. The variables were found to be the following:

x = 0,0004218
y = -0,0002261
z = 0,0016383
t = -0,0001742

Where x is assigned to chromium, y to nickel, z to manganese, t to molybdenum.
The constant in the equation for the upper boundary as seen in equation (17) dependence on the steel composition can thus be expressed as in equation (16).

$$k = 0{,}0004218 \cdot Cr(wt.\%) - 0{,}0002261 \cdot Ni(wt.\%) + 0{,}0016383 \cdot Mn(wt.\%) - 0{,}0001742 \cdot Mo(wt.\%) \quad (16)$$

$$\%C = k \cdot \frac{dC}{dt} \quad (17)$$

6.3 CO and CO_2 measurements by the new and old sample points

The CO and CO_2 content in the exhaust gas channel during the decarburization were plotted. The plots in figure 6.3.1-6.3.2 feature measurements using the old and new sample point.

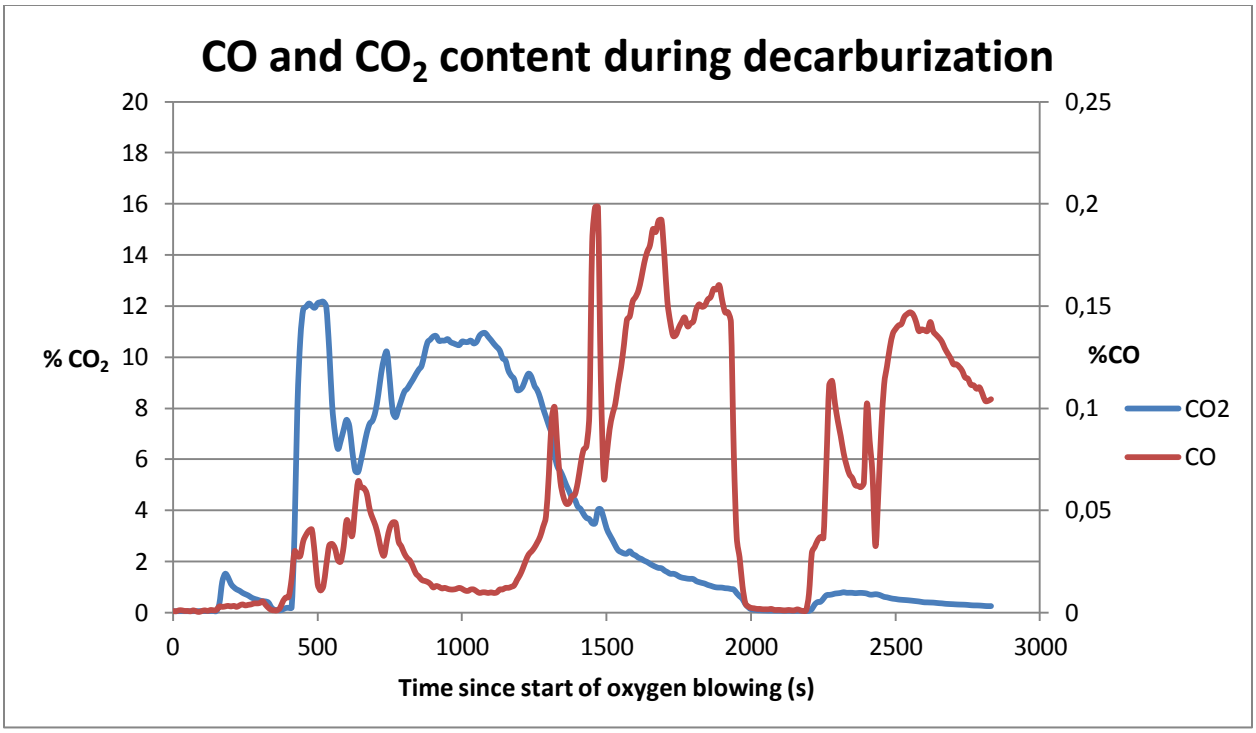

Figure 6.3.1: CO and CO_2 content during decarburization using the new sample point.

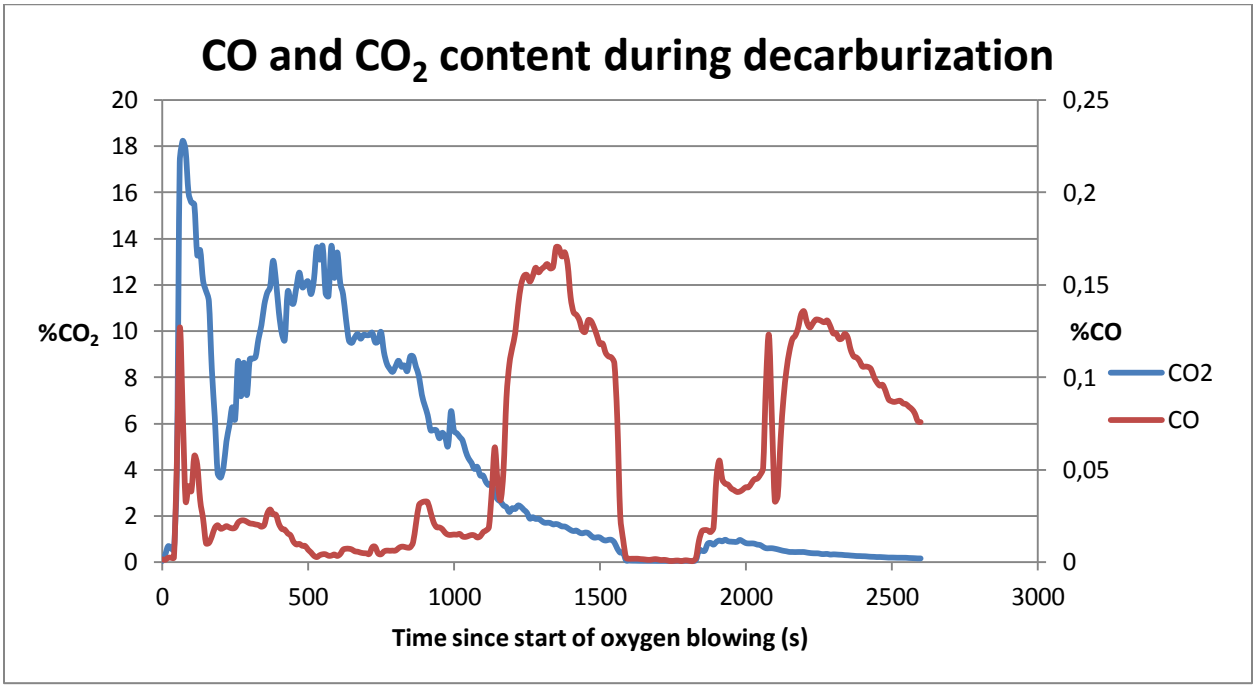

Figure 6.3.2: CO and CO_2 content during decarburization using the old sample point.

6.4 CRE

The CRE for the charges with the fastest and slowest decarburization were investigated for steel grades S32205, 304L and 316L. The average CRE of the first step was calculated and compared between the charges. Charges with the fastest and slowest decarburization and approximately the same delay were compared against each other. In three of the comparisons the charges with a fast decarburization had the highest CRE number during the first step. In one comparison, however, the charge with a slow decarburization had the highest average CRE during the first step. At what CRE the step changes occurred was also investigated and compared between the charges. Same charges were compared against each other. In three of the comparisons the step change occurred at a higher CRE for the charges with slow decarburization. In one comparison the step change occurred at a higher CRE for the charge with fast decarburization. Plots 6.4.1 and 6.4.2 illustrate the CRE plotted over the whole decarburization. The vertical lines represent the time of the step changes. At certain time intervals when the oxygen blowing is stopped there is no measured CRE. This is because the CRE is defined as the total amount of oxygen reacting with carbon divided by the total amount of blown oxygen. When the amount of blown oxygen is zero the CRE is undefined.

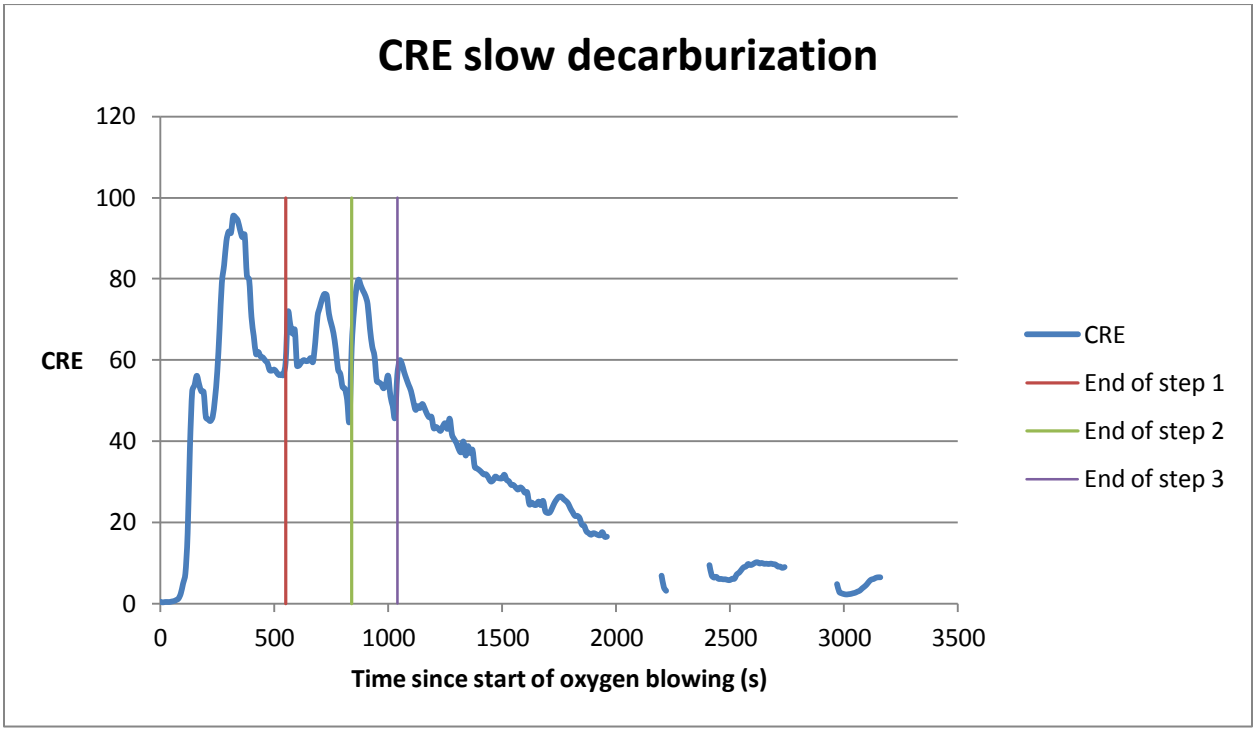

Figure 6.4.1: Plot of the CRE during decarburization for a charge with slow decarburization. The discontinuity represents a pause in the oxygen blowing.

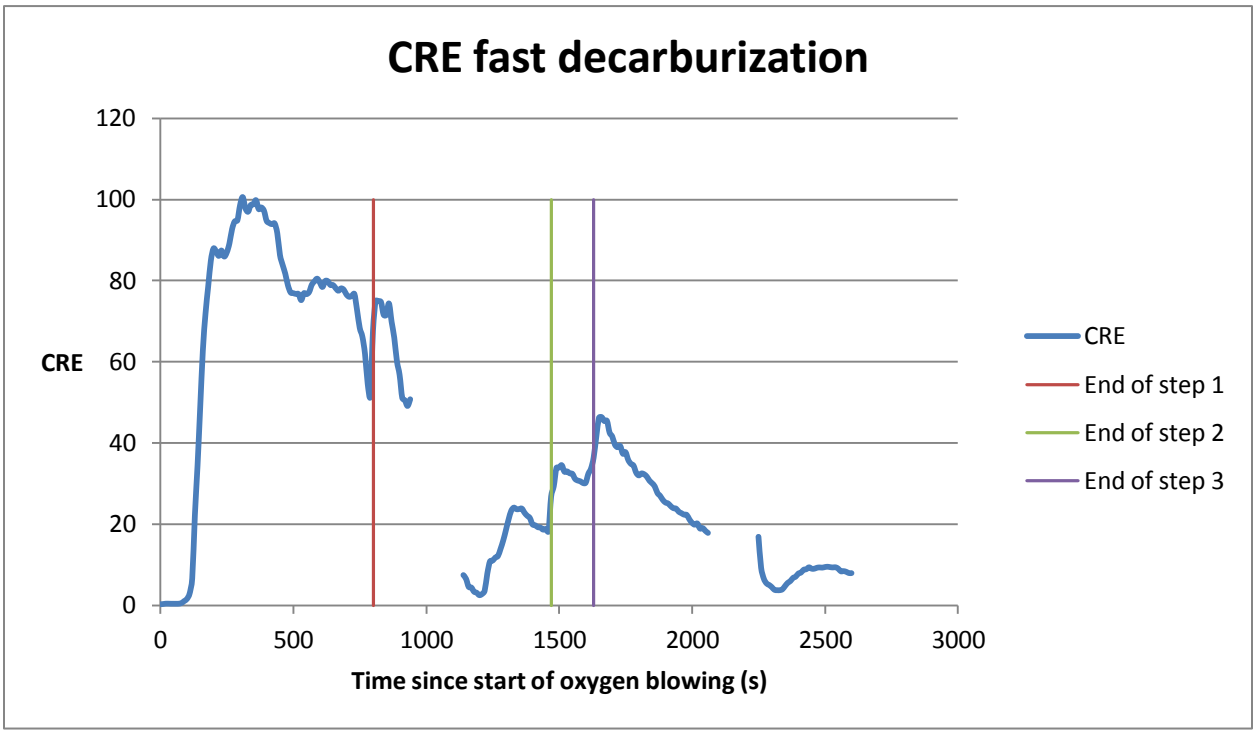

Figure 6.4.2: Plot of the CRE during the decarburization for a charge with fast decarburization. The discontinuity represents a pause in the oxygen blowing.

6.5 Mass balance

The correction factor in equation (13) was calculated for all charges which were included in this master thesis. The correction factor varied greatly between the charges when the carbon sample was taken during the last step. It could vary over 10% between subsequent charges of the same steel grade, which means that the error of the carbon prediction would be 10% of the initial carbon content before the decarburization began. However, for the charges where the carbon sample was taken at the end of step 3 the correction factor varied much less between subsequent charges. For steel grade S32205, when carbon samples were taken at the end of step 3, the standard deviation when using the mass balance was investigated. The correction factor of the previous charge was used in the mass balance calculations of the next charge. The standard deviation was found to be 0,0264 %C. Carbon samples were also taken at the end of

step 3 for steel grade S30815, but data from too few subsequent charges was available for applying to the mass balance model.

7. Discussion

For three out of the four steel grades which had carbon samples taken at the end of step 4 the IR-spectrometer gave the most accurate measurements at carbon contents below 1%. For steel grade 304L the mass spectrometer had the lowest standard deviation even at carbon contents below 1%. This was only due to the sample marked as a red square in the plot, which deviated the most. If not included the IR-spectrometer would have given the smallest standard deviation.

The linear regression between dC/dt and the carbon content proved to be more exact than the linear regression between dC/dt and the carbon activity. The contents of the alloying elements were taken from UTCAS theoretically calculated values. If samples would have been taken and the alloying element's actual contents would have been known the linear regression featuring the activity could have been more precise. However the purpose of the carbon prediction model is to avoid taking samples during the process. The contents of the alloying elements would therefore need to be taken from UTCAS during the process.

The amount of samples when the CO_2 content was under 1% for the different steel grades varied between 20 and 30. Ideally there would have been more carbon samples of every steel grade to be more confident in the results. With few samples every single deviating sample can have a great effect on the results.

In the measurements for the old sample point the probe was broken off and was therefore not situated in the center of the exhaust gas channel as it is supposed to be. The inner radius of the exhaust gas channel is approximately 1.3 m at the section where the old sample point is located. The probe should therefore also be 1.3 m in order to be situated in the center of the channel. It was however only 6 cm. It could cause measurements to be less reliable. At the end of the master thesis a new probe was installed. If a carbon prediction model would be developed for the old sample point with the new probe it could be compared to the carbon prediction model developed for the new sample point in this master thesis. It could then be decided which sample point is the most accurate. However, when the new probe was installed there was not enough time left to develop such a model in this master thesis.

The CRE study proved to be difficult. To see if fast or slow decarburization could be predicted by CRE measured online, charges of fast and slow decarburization needed to be compared. The comparison though is difficult to make due to many varying factors between the charges which affect the CRE value. The initial carbon content has a big effect because a high carbon content will increase the carbon removal efficiency. Cooling scrap is usually added one or several times during the decarburization and this means an interruption in the blowing and the CRE

measurements. It is difficult to compare two charges when they have interruptions in the blowing at different parts of the process.

The mass balance study on steel grade S32205 during step 3 showed that it was nearly as precise as the linear regression model. The correction factor of the previous charge was used in the mass balance calculations for the next charge. In practice, however, no carbon samples will be taken during step 3 for most steel grades. Carbon samples are only taken at step 3 for high carbon steel grades. The mass balance model requires calibration of the correction factor from the previous charge. It means that there would not be any calibration for the first charge in a sequence. The high carbon steel grades are not so common at Avesta Works either, which means that there are not usually many high carbon steel grades in a consecutive sequence. The mass balance therefore has limited potential benefits for use at step 3 in the AOD-process.

7.1 Sources of error

There are many sources of errors which affects the calculations in the exhaust gas analysis. The measuring errors of the analyzing equipments are given by the manufacturer. However, it is not clear if there are any additional measuring errors due to the installation and calibration of the equipment. There are also other sources of errors which have not been considered in the calculations. Entrained air will change the composition of the exhaust gas and some extra CO and CO_2 will enter the exhaust gas channel. The atmosphere's content of CO is however so low that it can be disregarded. The atmosphere's content of CO_2 is 390 ppm which is very low compared to the CO_2 due to the decarburization. However, in the end of the decarburization it will have a small effect. Other factors which affect the calculations have not been estimated. These factors include carbon which exits the converter in form of dust, carbon which ends up in the slag, and carbon which dissolves from the converter lining. If it always was the same amount of carbon it would not disturb the model's predictions, but it most likely differs from charge to charge.

8. Conclusions

When the CO_2 content in the exhaust gas channel is below 1% the IR-spectrometer gives more reliable measurements than the mass spectrometer. The equations which are based on the measurements by the IR-spectrometer should therefore be used in the production when the CO_2 content is below 1%.

Until the CO_2 content is below 1% the models based on the CO_2 measurements by the mass spectrometer can be used. For steel grade S32205 a separate equation for step 3 can also be used.

The linear regression model which is based on the correlation between dC/dt and carbon content gives a lower standard deviation than the model based on the correlation between dC/dt and the activity.

The new sample point has approximately 20 seconds longer delay than the old sample point. The delay for the new sample point is approximately 60 seconds as it was measured in this master thesis.

The R^2 factor in the plots was rather low and the standard deviation is high compared to the final carbon content. The samples in plots were rather scattered and it is therefore not possible to find an equation which perfectly describes the correlation between the carbon content and dC/dt.

A correlation between the composition of the steel during the decarburization and the constant in the upper boundary equation was found, equation (16). This equation could be used in the production for the four steel grades it was developed for. However, it needs to be tested on additional steel grades since it was only determined from four steel grades in this master thesis. It cannot be tested on one of the steel grades which was used to derive the equation. If it is found to be valid for additional steel grades it can eventually be used for more steel grades or possibly even for all steel grades. However, the equation seems reasonable from practical experience. According to it Cr and Mn decreases dC/dt and Ni and Mo increases it.

The upper boundary equation can be used to determine when to end the last step. When it predicts the carbon content to be the desired final content, the blowing can be stopped. 80% of the charges will then be under the predicted content, if not considering the measurement delay. The final carbon content is given as an interval with the aimed carbon content being in the middle. Even if 20% of the charges would have a higher carbon content than the aimed value it could still be within the acceptable interval. If too many charges would have a too high carbon content anyway it is possible to keep blowing a bit longer. It is preferred to blow longer to be sure that the carbon content is low enough, than to risk to end it too early. This is because

it is easier to add carbon afterwards than to start the decarburization again when additions have been made for the reduction and sulfur removal steps.

The upper boundary equation requires longer time to show the aimed carbon content than Excel's calculated linear regression formula by the least squares method. This is because it is designed to show a value which in 80% of the cases is higher than the actual carbon content to be on the safe side. For the upper boundary equation to show the aimed carbon content a longer blowing time is therefore needed. For an average charge, the extra blowing time before the upper boundary equation shows the aimed carbon content compared to Excel's linear equation was found to be approximately:

- 70 s for steel grade 304L
- 60 s for steel grade 316L
- 150 s for steel grade S32201
- 20 s for steel grade S32205

This extra blowing time is far less than the time it takes to take a carbon sample for all of the steel grades, except for S32201 for which it is approximately the same. It would thus be beneficial to use in the production.

The measurements with gas extracted from the new sample point gives more accurate measurements than those from the old sample point. The old sample point should, however, be evaluated in a new study, since the probe has been changed after it was evaluated in this master thesis. In the new study the same IR-spectrometer, which is used for the new sample point, should be used for the old one. The difference would then only be in the sample point itself and not in the analysis equipment.

The mass balance model could possibly be used to predict the carbon content in the end of step 3. For steel grade S32205 where carbon samples were taken at the end of step 3 the standard deviation of the mass balance model was 0,0264 %C. Moreover, it was 0,0193 %C for the linear regression model. However, in the mass balance model the correction factor needs to be calibrated after each charge and a carbon sample is needed for that. The mass balance can therefore only be a viable option for high carbon steel grades.

An online measured CRE value during the decarburization could theoretically be of great value in the AOD process. It could be used to run the process more effectively and be used as a basis for when to change steps. Finally, it should however, be pointed out that the study on CRE in this master thesis was inconclusive.

9. Recommendations for further work

- Evaluate how well equation (16) works for determining the constant in the upper boundary equation, by testing it on other steel grades than those covered in this master thesis.
- Incorporate the exhaust gas analysis in the UTCAS model. Use both dynamical measurements from the exhaust gas analysis and UTCAS theoretical calculations. It would be a demanding project, but to improve the carbon prediction model the thermodynamics and kinetics in the converter would need to be considered.
- Develop a new carbon prediction model for the old sample point. When the model has been created for the old sample point it can be determined which sample point is the most accurate.
- Conduct a larger study on online measured CRE values to find out if it can be used to control the process.
- Alternative techniques for analyzing the exhaust gases can be evaluated. Online measuring methods could lower the measurement delay by up to 40 seconds.
- A filter needs to be added before the water separator to prevent dust from precipitating inside it.
- Install an automatic clean blowing system for the new sample point.

References

[1] http://www.outokumpu.com, visited 2012-04-16.

[2] Outokumpu's annual report from 2011.

[3]Private communications with Jyrki Pitkälä, Process developer at the AOD-converter at Avesta Works.

[4] Lecture notes from Robert Vikman in the course MH2044 Advanced course in process sciences at the Royal Institute of Technology.

[5] Process education at Onet, Outokumpu's intranet.

[6] Private communications with the operators at the AOD-converter at Avesta Works.

[7] T. Abel Engh, et al., "Principles of metal refining". Oxford University Press. 1992.

[8] Mikael Lindvall, et al., "Förbättrad styrning av AOD med avgasanalys och temperaturmätning". Jernkontoret, 2011.

[9] S. Ferranti, et al., "Dynamic process control of AOD converters". European commission, 2002.

[10] Pentti Kupari, "VKU2 ja AOD2 savukaasujen analysointijärjestelmät". Internal Outokumpu report, 2001.

[11] Internal documentation on exhaust gas analysis at the AOD-converter, Avesta Works.

[12] Erik Grånäs, "Prediction of the carbon content in the AOD converter by flue gas analysis". Royal Institute of Technology, 2004.

[13] Internal documentation on composition of the steel grades at Avesta Works.

[14]Private communications with Gunnar Lindstrand, metallurgist at Avesta Works.

[15] Mikael Lindvall, et al., "Aktuell teknik för bestämning av avgasanalys för on-line processkontroll". Jernkontoret, 2007.

[16] ABB EasyLine continuous gas analyzers EL3000 series, Manual for the EL3000 IR-spectrometer, revised 2008.

[17] The McCROMETER √CONE® Flowmeter, Manual for installation and operation, Revised 1992.

[18] McCrometer v-cone general brochure, 2009.

[19] Torbjörn Engkvist, "Mätosäkerthet – redovisning på analyslaboratoriet". Internal Outokumpu report, 2011.

[20] Zhigang Hu, "Continuous determination of bath carbon content on 150 t BOF by off-gas analyzer". Journal of University of Science Technology, volume 10, number 6, page 22, December 2003.

Acknowledgements

I would like to thank the following people for help during this master thesis:

Jyrki Pitkälä
Patrik Ternstedt
The operators at the AOD-converter
Anders Appell
Kjell Swed
Gunnar Lindstrand
Torbjörn Engkvist